THE
PHYSICAL REVIEW
A journal of experimental and theoretical physics established by E. L. Nichols in 1893

SECOND SERIES, VOL. 65, NOS. 9 AND 10 MAY 1 AND 15, 1944

The Average Ionization and Energy Loss of Cosmic-Ray Mesotrons in Air

WAYNE E. HAZEN
Department of Physics, University of California, Berkeley, California
(Received March 27, 1944)

The average specific ionization of cosmic-ray mesotrons has been determined at sea level and at 100 feet underground from drop counts along diffuse cloud-chamber tracks. The cloud chamber was operated in such a way that the efficiency of condensation on ions was known. The average specific ionization, excluding energy transfers greater than 800 ev, is essentially 50 ion pairs per cm of air at N.T.P. for both locations. Since a 15 percent increase is expected for the measurements underground, it is suggested that the high energy cosmic rays may be protons. If all energy transfers less than 10^4 ev are included, the average energy loss is 1.35×10^3 ev per g/cm^2 of air, in reasonable agreement with the theory. The observed cross sections for energy transfers between 800 and 3200 ev agree with the Rutherford formula when the electron binding is taken into account.

THE energy loss of ionizing cosmic-ray particles in gases is determined indirectly from ionization measurements. For mesotrons the energy loss in air from nuclear (radiative) collisions is negligible for energies less than 10^{11} ev;[1] since more than 98 percent of the mesotrons at sea level have energies[2] less than 10^{11} ev, radiation loss can be neglected. The total number of ions produced by *low energy* ionizing rays of known energy has been measured by several different methods.[3] The average energy loss per ion pair is independent of the energy of the primary particle and has a value of 32 ev per ion pair for air. Since the entire energy of even a cosmic ray is ultimately dissipated in low energy transfers, it is reasonable to assume that the factor, 32 ev per ion pair, can be used in converting from ionization to energy loss in the case of cosmic rays.

Several measurements, both of the primary ionization and of the "total" ionization, have been made in a variety of gases and by several different methods.[4,5] The determinations of primary ionization, which have been made from cloud-chamber photographs and from counter efficiency measurements,[4] are relatively accordant.[6] But the measurements of total or probable ionization give discordant results.[4,5] The values obtained by combining ionization chamber and counter measurements (i.e., division of the total number of ions formed per sec. per cm^3 by the number of particles traversing a unit volume per sec.) are subject not only to the uncertainties in the results of each of the two types of experiments, but also to the uncertainty in establishing the applicability of the counter data to the ionization chamber environment. The pulse-ionization chamber method is subject either to

[1] H. J. Bhabha, Proc. Roy. Soc. **A164**, 257 (1938).
[2] P. M. S. Blackett, Proc. Roy. Soc. **A159**, 1 (1937).
[3] H. Eisl, Ann. d. Physik **3**, 379 (1929). C. E. Nielsen, Ph.D. Thesis, University of California (1941).
[4] T. H. Johnson, Rev. Mod. Phys. **10**, 193 (1938).
[5] R. B. Brode, Rev. Mod. Phys. **11**, 222 (1939).
[6] W. E. Hazen, Phys. Rev. **63**, 107 (1943).

many experimental difficulties or to uncertainties in the interpretation of the data and, as a result, only one really quantitative experiment has thus far been performed.[7]

Only a high pressure ionization chamber measures a value for the ionization approximating the total ionization. In low pressure ionization chambers many of the ions are undetected because they occur along the tracks of secondaries of range greater than the chamber size; in cloud chambers a relatively short total track length is observed and the infrequent high energy transfers are not likely to be observed. With the cloud chamber, therefore, it is possible to obtain values for the ionization that include collisions in which the cosmic ray loses as much as several thousand electron volts with a reasonable number of pictures, but a determination of the total ionization might require many thousand. In the present experiment the average ionization of mesotrons has been determined at sea level and under 100 feet of rock. From these figures we can obtain a value for the average energy loss of mesotrons in air that includes all collisions in which 10^4 ev or less are lost by the mesotron in a single encounter.

The theory of ionization and energy loss of high speed charged particles leads to the prediction that both quantities increase with the energy of the high speed particle when its kinetic energy is greater than three times its mass energy. Direct measurement of the increase in primary ionization with energy was first attempted by Kunze,[8] but with negative results. His results have since been explained by the fact that he was observing mesotrons rather than high energy electrons. A study of the ionization by cosmic-ray electrons by Corson and Brode[9] indicates a rise in ionization with energy but their results involve a large uncertainty concerning the efficiency of condensation on ions. Sen Gupta[10] performed a similar experiment with a technique stated to be similar to that of Corson and Brode and with a magnetic field strong enough to deflect some of the mesotrons and protons. There was an indication of an increase in ionization with energy for the electrons, but only a slight increase for the mesotrons. Either the drop images were poorly resolved or the condensation efficiency was low since the observed average ionization for mesotrons was only 40 ion pairs per cm in air at N.T.P.

Experiments on the energy loss of mesotrons in metal plates[11] also indicate an increase with energy, but the increase was not significantly greater than the experimental uncertainty. A previous experiment by the author[6] showed that the average primary ionization by mesotrons was no higher than the minimum ionization by electrons, whereas calculations predicted a value at least ten percent higher.

In the present experiment we have a comparison of the average ionization by two groups of mesotrons, one with a much higher average energy than the other, and we should expect to find an increase in average ionization for the group with the higher average energy.

EXPERIMENTAL METHOD

The first pictures were taken in the downgrade fresh-air duct of the Broadway Low Level Tunnel in Oakland, California, at a depth of 100 feet (a few pictures were obtained at 400 feet). The lower half of the 30 by 30 cm cylindrical chamber contained four lead plates, but this portion of the cloud chamber was not photographed in all of the expansions. The upper portion of the chamber contained an electrode system that supplied a uniform horizontal electric field normal to the chamber axis—thus, by delaying the expansion an appropriate length of time, the cosmic-ray "track" becomes a pair of separated diffuse columns of ions, one positive and the other negative.

When the expansion is completed, some of the ions act as nuclei for drop formation. Studies of the condensation efficiency of the ions,[3,12] indicate that, with ethanol-water mixtures in the neighborhood of the ratio 3:1, over 95 percent of the plus ions form drops when the observed ratio of minus to plus drops is 1:10 and is essentially 100 percent when the ratio is greater than 1:5.

[7] W. C. Dunlap, Ph.D. Thesis, University of California (1942).
[8] P. Kunze, Zeits. f. Physik **83**, 1 (1933).
[9] D. R. Corson and R. B. Brode, Phys. Rev. **53**, 773 (1938).
[10] R. L. Sen Gupta, Nature **146**, 65 (1940).
[11] J. G. Wilson, Proc. Roy. Soc. **A172**, 517 (1939).
[12] G. D. Bagley, Phys. Rev. **56**, 851A (1939).

Since the alcohol diffuses through the rubber diaphragm and must be replenished periodically, the mixture usually is not in the ratio 3:1. Nielsen also made a few measurements with ethanol-water mixtures containing 40 percent and 87 percent ethanol. These measurements show that the condensation efficiency is certainly very close to 100 percent in the vapor from the above mixtures when the observed ratio of minus to plus drops is greater than 1:2. In the present experiment the ratio of drops in the minus and plus ion columns was used as the criterion for condensation efficiency on plus ions.

Counter control was obtained from four counter tubes in double coincidence placed above the chamber; the counting rate was one in three minutes at a depth of 100 feet. A seven-centimeter thickness of lead was placed above the counters in order to distinguish between the soft and the hard component; photographs with more than one track were discarded since, although nearly all such events consist of a mesotron accompanied by an electron, it is usually impossible to identify the mesotron in such cases. Ordinarily it is necessary to place lead below the counters in order to detect cases in which a divergent knock-on electron from the upper lead plate trips the counters, but in this experiment the cloud chamber was so large that the mesotron also would be observed.

Since the chamber was expanded by a relay, which introduced a delay in the expansion, and the expansion itself was relatively slow, no additional time delay was necessary in order to produce sufficiently diffuse tracks (2.5-mm diameter). The clearing field was maintained at 20 volts/cm until shorted by the coincidence-circuit relay. The delay inherent in the clearing-field relay permitted a separation of the plus and minus ions by six or seven millimeters before the clearing field fell to zero. Figure 1 shows one of the tracks as an example.

Illumination was provided by two argon flash tubes, each of which was mounted slightly outside the focal point of a set of condensing lenses. The beams of light were directed forward at an angle such that the light reaching the camera was scattered by the drops through an angle of $\sim 55°$. The flash tubes used in this experiment are the most satisfactory light source ever employed in this laboratory;[13] the lumen-second output during the exposure is at least as great as that for any other type of source, and the average life is roughly 1000 flashes. With exposures at f:18 and a magnification of 0.157, the depth of focus was four centimeters for a circle of confusion less than 0.002-cm radius (the minimum circle of confusion was 0.001 cm).

FIG. 1. An enlarged section of one of the mesotron tracks. The ions not only have diffused but also have separated into columns of plus and minus ions before the drops formed. The denser column of drops formed on the plus ions. The actual length of the portion of the original track here reproduced was 4 cm.

In the case of the experiments at sea level, the lead plates were removed and the 30 by 30 cm cylinder was replaced by a 30 by 45 cm cylinder. The transverse clearing field was thus extended to include a 30 by 30 cm cylindrical region; the rear third of the glass cylinder was left free for the

[13] The flash tubes and accompanying circuits were developed by Dr. Eugene Gardner in connection with another experiment.

entrance of the light beam. Single counters were placed above and below the chamber with the lead above the upper counter.

Johnson[4] mentions three objections to the cloud-chamber method of determining specific ionization along diffuse tracks: (a) poor resolution in the clusters, (b) unobserved ionization at a distance from a track, resulting from x-ray excitation, and (c) recombination of ions in the absence of any electric field. (a) In the present experiment, all clusters that were not well resolved in the plus column were counted in the less dense minus column, and the result was multiplied by the ratio of plus to minus drops in the neighboring lengths of track. The energy, and thus the ionization, in branches with appreciable range, were obtained from a measurement of the range (there was no magnetic field which would deflect the branch electrons). (b) The calculated distance for absorption of one-half of the oxygen x-rays is only 3 mm according to Nielsen[3] and observations, both by Nielsen and by the author, have never given evidence for

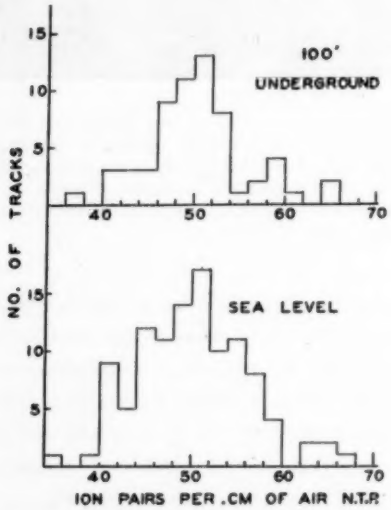

FIG. 2. Block diagrams showing the frequency distributions in the data for the specific ionization of cosmic-ray mesotrons. The mean value is 50 for the upper curve and 51 for the lower curve. The abscissae can be changed to electron volts by multiplying by the factor 32 ev/ion pair.

ionization clusters noticeably separated from a diffuse track. (c) In the present experiment there was an electric field to separate the ions.

The source of the greatest uncertainty in the cloud-chamber method has usually been the uncertainty in condensation efficiency. This is probably the case in the present work.

EXPERIMENTAL RESULTS

The drop counts were made on the negatives themselves with a comparator microscope. The number of drops in the positive column averaged ~700 per track for the Broadway Tunnel photographs and ~1000 per track for the sea level photographs. Clusters of drops numbering 25 or more (the actual clusters contained 40 or more drops but the average ionization was 15 in the length of track occupied by a cluster) were considered apart from the general drop count. It was found that statistical variations from one track to the next were greatly reduced when larger clusters were excluded, but on the other hand the criterion for exclusion was applied so infrequently that no appreciable error resulted from cases where the cluster size was $\simeq 25$.

In order to reduce the data to number of drops per cm at N.T.P., factors involving temperature, pressure, and magnification were considered. A fiducial magnification was established photographically at a distance approximately the same as the original track distances; the distance and inclination angle (small for the Broadway Tunnel tracks, negligibly small for the sea level tracks) of individual tracks were determined by reprojection, and the magnification was calculated for each track. Block diagrams of the distributions for both sets of data are given in Fig. 2.

The average ionization is 51 per cm at sea level, and it is 50 per cm 100 feet underground. The statistical uncertainty in the ionization of an individual track is determined essentially by the number of primary ionization events, which is 20 per cm in air or 40 percent of the ionization observed in the present experiment. The probable statistical deviation in the ionization of an individual track is thus: $0.67\times 50/(0.4\times 1000)^{\frac{1}{2}}=1.7$ ions per cm at sea level and 2.0 ions per cm 100 feet underground. Both distribution curves are many times broader than would be expected on the assumptions that the main uncertainty is statistical variation in the ionization and that each track is a measurement of the same quantity. Without doubt neither assumption is justified.

The energy loss in electron volts represented by a given number of ion pairs is obtained by

multiplying the number of ion pairs by 32. As noted above, clusters of 25 or more drops were recorded as separate events, i.e., each collision in which the mesotron lost 800 or more ev was listed. In the sea level drop counts, the total

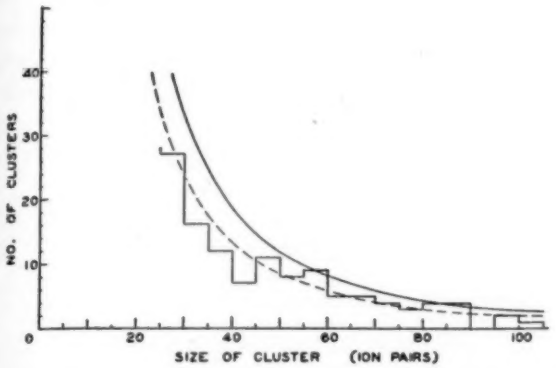

FIG. 3. Frequency distribution for clusters of ions in the tracks of cosmic-ray mesotrons. Each cluster arises from a collision in which a mesotron transfers to an electron an energy (in electron volts) of 32 times the cluster size. The solid curve is given by the Rutherford formula on the basis of free electrons; the dashed curve, by the same formula for bound K electrons.

number of ion pairs occurring in clusters of 25 to 310 was 7620, whereas the total number of ion pairs excluding clusters larger than 25 was 96,000. Thus the average ionization including energy transfers up to 10^4 ev (clusters up to 310) is 51 increased by 7620/96,000 or 54 ion pairs per cm in air at N.T.P. The corresponding energy loss is 1700 ev/cm or 1.35×10^6 ev per g/cm² of air. In Fig. 3 is given a frequency distribution for the energy losses greater than 800 ev.

INTERPRETATION OF RESULTS

The theoretical value for the minimum energy loss[14] is 1.28×10^6 ev per g/cm² in air for energy transfers less than 10^4 ev. Since the average energy loss is certainly somewhat higher than the minimum energy loss, we can consider the agreement with the measured value of 1.35×10^6 as satisfactory.

The expected average ionization for a group of mesotrons is

$$\int I(E)\cdot f(E)\cdot dE/\int f(E)\cdot dE,$$

where $I(E)$ is the specific ionization for energy E, and $f(E)$ is the relative number of mesotrons with energy E to $E+dE$. Since $f(E)$ has actually been determined as $f(H\rho)$, it is more convenient to perform the numerical integrations in terms of $H\rho$ (all values of $H\rho$ will be given in gauss-cm). The spectral distribution $f(H\rho)$ obtained by Blackett[2] extends down to $H\rho=1.7\times10^6$ without corrections. Three lower points on the curve were obtained from: (1) Blackett's data for the number of particles in the range of $H\rho$ from 7×10^5 to 1.7×10^6, multiplied by the correction factor 3.28 to allow for the exclusion of particles by the magnetic field;[2] (2) Greisen's figure[15] of 0.08 for the fractional number of mesotrons in the $H\rho$ range 1.7×10^5 to 8.3×10^5; and (3) the isolated point given by Williams[16] at $H\rho=1.2\times10^5$. For values of $H\rho$ greater than 10^8, the spectrum is not known from direct measurements, but absorption measurements and other types of evidence lead to the assumption of a $1/E^3$ distribution. Fortunately, the calculated average ionization does not depend critically on the values of $f(H\rho)$ at low and high values of $H\rho$.

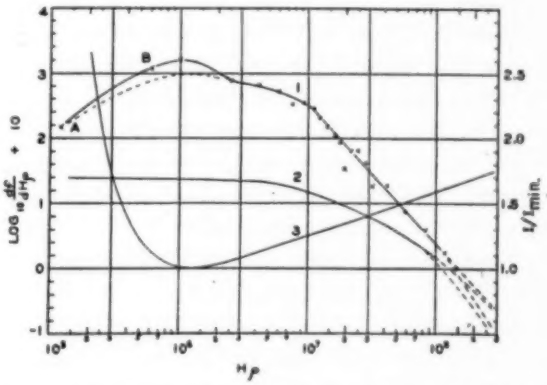

FIG. 4. Curves used in the integrations to obtain the expected average specific ionization of mesotrons. Curve *1* is the energy spectrum at sea level according to Blackett (points *A* and *B* are from data of Williams and Greisen, respectively). Curve *2* is the energy spectrum 100 feet underground, under the assumption that all of the particles lost 10^{10} ev in traversing the rock. On the ordinate scale for curves *1* and *2* (left), df is the relative number of particles in the $H\rho$ range $H\rho$ to $H\rho-dH\rho$. The dotted portions of curves *1* and *2* represent possible variations in the curves that arise from uncertainties in the measurements. Curve *3* is the ionization curve (scale of ordinates at the right).

Figure 4 shows the curves used in the numerical integrations. The curve for the spectrum 100 feet underground was obtained from the sea

[14] B. Rossi and K. Greisen, Rev. Mod. Phys. **13**, 240 (1941).

[15] K. Greisen, Phys. Rev. **63**, 323 (1943).

[16] E. J. Williams, Proc. Roy. Soc. **A172**, 206 (1939).

level spectrum by assuming that all of the rays lost 10^{10} ev of energy in penetrating to the tunnel. There are two reasons for not considering the variation in energy loss with energy in determining the underground spectrum: The results are not appreciably altered, and the present experiment indicates no variation with energy. The results of the integrations are $I_0 = 1.18 \cdot I_{min}$ (at sea level) and $I_{100} = 1.42 \cdot I_{min}$ (at the tunnel). When variations that are believed possible are made at the lower and at the upper end of the spectra, the results are changed by two percent or less. Thus we are led to expect an increase of at least 15 percent in the average ionization when 100 feet of rock filter is added, whereas the experimental values for the average ionization are essentially identical. The frequency distributions (Fig. 2) are broader than one would expect from statistical fluctuations alone, but it seems highly unlikely that any experimental errors could mask a 15 percent difference in the means of the two distributions.

There are several possible phenomenological explanations, among which are: (1) the ionization does not increase with energy more than one-fourth as rapidly as the predicted increase; (2) the polarization effect takes place at energies lower by a factor of 50 than Fermi calculates;[17] or (3) most of the particles with $H\rho > 10^7$ are protons. The first possibility is not very likely since the increase in ionization is predicted on the basis of supposedly well-established precepts, and since available experimental results, although subject to large uncertainties, agree with the predicted rise. The second is also unlikely even though the theoretical calculations are admittedly rough. The third is not generally accepted, but other experimental evidence is not overwhelmingly against such a possibility; if true, some 30 percent of the hard component might consist at sea level of protons.

The frequency distribution for clusters and delta-rays of energy greater than 800 ev in the sea level tracks is given in Fig. 3. The total number of such collisions was 135 in a total track length of 1930 cm. The Rutherford formula applies to the types of collisions included in this study as far as considerations of spin, relativity, collision time, etc., are concerned,[14] but the assumption of free electrons is not justified for the two K electrons of oxygen or nitrogen in the lower energy collisions. However, the correct collision cross section is somewhere between that obtained by assuming all the electrons as free and that obtained by assuming the K electrons cannot be removed.

The Rutherford formula (for free electrons) with the constants evaluated is

$$N(E)dE = 98dE/E^2 \text{ cm}^{-1} \text{ ev}^{-1},$$

where $N(E)$ is the number of collisions in which energy E to $E+dE$ is lost by the mesotron per cm of air at N.T.P. For completely bound K electrons the factor 98 would be reduced to 71. The theoretical curve is a fairly satisfactory representation of the data when the K electrons are considered free for the higher energies and bound for the lower energies. Several groups[18] have measured the frequency of occurrence of collisions with much higher energy transfers (more than 10,000 ev). Hornbeck and Howell found reasonable agreement with theoretical calculations for the case of electrons. Seren has shown that the Rutherford formula agrees with experiment for the frequency of mesotron collisions resulting in energy transfers greater than 13,000 ev.

In general, there seems to be reasonable agreement between theory and experiment for the ionization by high speed particles, except for the comparison of the average specific ionization by filtered (100 feet of rock) and unfiltered penetrating rays.

The author is greatly indebted to Mr. F. I. Doane of the State Highway Department for permission to work in the Broadway Low Level Tunnel and for his general cooperation.

[17] E. Fermi, Phys. Rev. **57**, 485 (1940).

[18] G. Hornbeck and I. Howell, Proc. Am. Phil. Soc. **84**, 33 (1941); L. Seren, Phys. Rev. **62**, 204 (1942).

Isotope Shift in Magnesium*

L. G. MUNDIE AND K. W. MEISSNER
Purdue University, Lafayette, Indiana

(Received January 15, 1944)

The previous investigations concerning the isotope shift of magnesium have been repeated and extended by means of an improved atomic beam source and a Perot-Fabry interferometer. The values of Meissner have been checked to within experimental error in most cases. In addition, several new lines have been resolved, and their isotope shifts determined. The $3\,^1P-m\,^1D$ series has been resolved from $m=3$ out as far as the member $m=11$. In this series the values of $\Delta\nu(=\nu_{26}-\nu_{24})$ seem to converge to a value of about 0.068 cm^{-1} rather than the value 0.056 cm^{-1} obtained by Meissner. The isotopic shifts of the members $m=5$ and $m=6$ of the series $3\,^1P-m\,^1S$ have been measured. The results obtained are discussed in connection with the theoretical work of Vinti, who assumed the splitting to be solely a mass effect. The experimental and theoretical values of $\Delta\nu$ agree in sign, but the former are usually larger by a factor of about two. The $3\,^2D-4\,^2F$ doublet of Mg II at 4481A has been measured very carefully and the separation of the two components found to be 1.000 ± 0.002 cm^{-1}.

INTRODUCTION

THE magnesium atom is ideal for the study of isotope shift. It possesses three isotopes of mass numbers 24, 25, and 26, and abundance percentages 77.4; 11.5; 11.1. Since the atomic number is even, no nuclear spin is to be expected for the isotopes 24 and 26. It can further be shown[1] that the isotope 25 is not likely to cause observable hyperfine splitting in many of the most prominent lines because of the nature of the states involved.

It may be advisable to give a brief résumé of earlier investigations of the magnesium spectrum.

Murakawa[2] investigated the problem using a water-cooled Schueler discharge tube and found all lines sharp and single.

Bacher and Sawyer[1] repeated the investigation using a liquid-air-cooled Schueler tube. Their spectral apparatus consisted of a Perot-Fabry interferometer in combination with a glass spectrograph. Values of plate separations up to 29.5 mm were used. All of the lines investigated, with the exception of the strong triplet 5183/72/67A ($3\,^3P_{2,1,0}-4\,^3S_1$), were found to possess two components, a strong one, and a considerably weaker satellite on the short wave-length side.

These observations were interpreted by Bacher and Sawyer as an isotope effect. The explanation of the structure as a pure mass effect was eliminated because of the presence of only one satellite, instead of two. It was also pointed out that the shift was in the wrong direction to be accounted for by a difference in nuclear fields caused by the fact that the nuclei with a larger number of particles have larger radii. The fact that only two components were observed was explained as directly due to perturbation effects. The splitting was found to be quantitatively related to the magnitude of the perturbation.

The investigation was extended to the resonance line by Jackson and Kuhn[3] and by Fisher[4] using the atomic beam in absorption and emission, respectively. Both investigations revealed again two components, the weaker lying on the short wave-length side. The magnitude of the splitting obtained was quite different in the two cases, however; Jackson and Kuhn obtained the value $+0.033\pm0.002$ cm^{-1}, while Fisher reported a splitting of $+0.066$ cm^{-1}.

Meissner[5] repeated the investigation employing the atomic beam as a light source. A Perot-Fabry interferometer was used with separations of 12, 36, 42, 60, and 180 mm. His spectrograms exhibit an entirely different appearance from those of earlier workers. With the exception of

* Based upon a thesis submitted by L. G. Mundie to the faculty of Purdue University in partial fulfillment of the requirements for the degree of Doctor of Philosophy in April, 1943.

[1] A. E. Bacher and R. A. Sawyer, Phys. Rev. **47**, 587 (1935).

[2] K. Murakawa, Zeits. f. Physik **72**, 793 (1931).

[3] D. A. Jackson and H. Kuhn, Proc. Roy. Soc. **A164**, 48 (1938).

[4] R. A. Fisher, Phys. Rev. **51**, 381 (1937).

[5] K. W. Meissner, Ann. d. Physik **31**, 505 (1938).

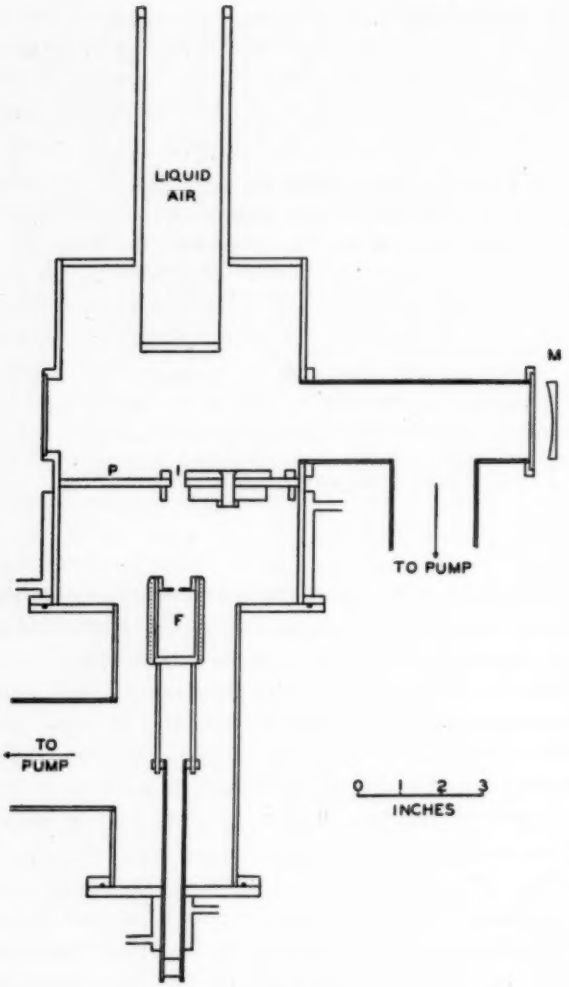

FIG. 1.

the green triplet at 5183A, all of the more intense lines were found to consist of *three* nearly equally spaced components. The strongest component was of longest wave-length; the other two were of nearly equal intensity. The explanation as a pure mass effect was of course strongly suggested, and hence proposed by Meissner. The line shifts of the $3\,^1P-m\,^1D$ series were observed from $m=3$ to $m=7$. Convergence of the latter values allowed a calculation of the isotope shift of the $3\,^1P$ term, as well as the $m\,^1D$ terms involved. The shift of the $5\,^1S$ term was also obtained. The analysis could not be pushed any further, however, because of lack of sufficient accurate experimental data.

Fisher[6] has recently repeated his work on the resonance line at 2852A. He succeeded in resolving the triplet isotope structure and found the separation from the main component of the two weaker components to be 0.030 and 0.053 cm^{-1}.

A theoretical investigation of the isotope shift in magnesium has been recently carried out by Vinti,[7] who assumes the shift to be solely a mass effect. The "specific" shift (that part of the total shift which is not accounted for by replacing m, the mass of the electron, by μ, the reduced mass, in the wave equation) is treated as a perturbation in much the same way as was done in the case of Li by Hughes and Eckart.[8] Only a first-order approximation is necessary, as the second approximation is smaller by a factor of the order m/M, where M is the mass of the nucleus. By choosing explicit radial functions, Vinti was able to calculate the splitting of several lines. The results obtained are of the right order of magnitude, but on the whole the agreement with the observed values is not particularly satisfactory. Using the observed values of $\Delta\nu$, Vinti was further able to predict the splitting of several other lines without making any explicit use of radial functions.

The present investigation was undertaken with the aim of repeating and extending the previous experimental investigations of isotope shift in magnesium. Such an undertaking is worthy of attention in view of the following facts:

(a) The results of Meissner are in complete disagreement with the results of earlier investigations; and (b) the agreement between theory and experiment is not particularly good. A confirmation of the earlier measurements was therefore desirable. Furthermore, there was hope that new and more extended experiments could give information about the isotope shift of lines which had not been investigated experimentally but which Vinti had calculated.

I. EXPERIMENTAL DETAILS

A. The Atomic Beam Apparatus

The prime requirement of an atomic beam for the present type of investigation is that it should produce a spectrum which (1) has sufficient intensity for the production of spectrograms in

[6] R. A. Fisher, Rev. Mod. Phys. **14**, 79 (1942).

[7] J. P. Vinti, Phys. Rev. **56**, 1120 (1939).

[8] D. S. Hughes and C. Eckart, Phys. Rev. **36**, 694 (1930).

reasonably short times, (2) has the freedom from Doppler broadening required in the particular case under investigation, and (3) is reasonably free from foreign lines and bands. Experimentally this means that we must have (1) the greatest possible density in both the atomic and the exciting electronic beams, (2) sufficient collimation of the atomic beam, and (3) a high vacuum in the excitation chamber.

It might be pointed out that the intensity requirements in the present case are rather high. This is seen when we consider that the intensity at the maximum of a fringe formed by a Perot-Fabry interferometer is of the order of only one percent of that of the incident light and that, furthermore, we are interested in bringing out satellites which are even many times weaker than the main component.

The vacuum requirement is also not easily fulfilled because of the enormous amounts of gas given off by the furnace, filament, anode, and the walls of the chamber which are under constant bombardment by stray electrons.

The apparatus finally evolved from a series of preliminary trials may be described in detail.

A general view of the arrangement is seen in Fig. 1. It consists of a cylindrical chamber which has been divided by the copper plate P into two parts: the furnace chamber, and the excitation chamber. Each of these is connected directly to an oil diffusion pump having a pumping speed of about 45 liters per second. The two chambers are joined only by the so-called image aperture I through which the atomic beam passes, prior to deposition on the base of the liquid air trap. With this arrangement an excellent vacuum can be maintained in the excitation chamber even while the furnace is giving off a considerable amount of gas. The furnace F consists of a steel cylinder wound with Nichrome V wire embedded in Saureisen cement. It is mounted on three long nickel-silver legs to minimize the conduction of heat to the support. The cover is recessed into the furnace cavity to ensure a high temperature of the oven aperture, and hence avoid deposition of metal upon it. The walls of the furnace chamber are water cooled. By use of the concave spherical mirror M so arranged as to form a real image of the beam at the beam itself, a considerable improvement in the intensity was obtained.

In order to avoid clogging of the image aperture I, the device shown in Fig. 2 was used. (This arrangement is also to be seen in cross section in Fig. 1.) Eleven slits 2 mm × 10 mm were cut in a circular brass plate B as indicated. These image apertures are brought into position over the oven aperture one after the other by means of a lateral motion of the lever L. Motion is allowed by the sylphon S, and restricted to the horizontal direction by the vertical pin P. The motion is transmitted to the plate by a pawl and ratchet arrangement. In order to avoid clogging of the stationary opening O in the dividing plate D, it was found necessary to introduce a second rotating plate A on the lower side of the dividing plate. The plate A is rigidly connected to B, and contains a set of corresponding slits considerably larger than those in B. It was found that about fifteen minutes were required for any appreciable clogging of an image slit. Thus the eleven slits were sufficient for even the longest exposure.

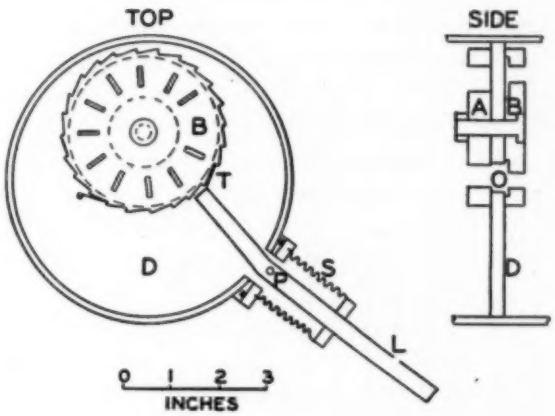

FIG. 2.

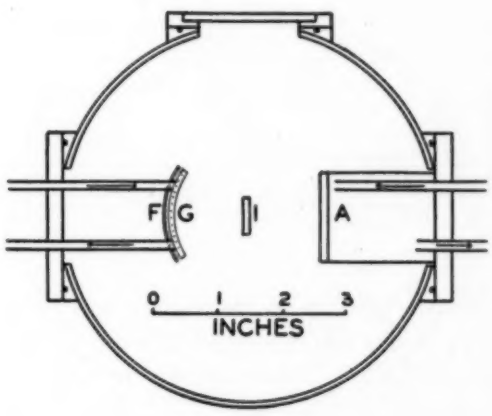

FIG. 3.

The final electron gun arrangement adopted was similar to that used by Meissner and Luft.[8,9] As a description of their arrangement has never been published, it will be described in detail here. The general arrangement is seen schematically in Fig. 3, which represents a top view of the assembled device. The filament F and grid G are in the shape of portions of concentric cylinders. The image slit I is located so as to send the atomic beam along the common axis of these cylinders. The water-cooled anode A collects the electrons that have passed through the excitation region, and assists in focusing the electrons. The leads of the filament are omitted in this sketch.

In Fig. 4 the details of the construction of the grid are shown. The grid elements consist of nickel tubes T of 0.045" O.D., and 0.009" wall thickness. Cooling is accomplished by passing distilled water along the paths indicated by the arrows. The nickel tubes are hard-soldered into the brass frame B, the profile of which is to be seen in the "front view" diagram. B is, in turn, hard-soldered between two thin copper frames C.

An Eastern centrifugal force pump was originally used for circulating the distilled water

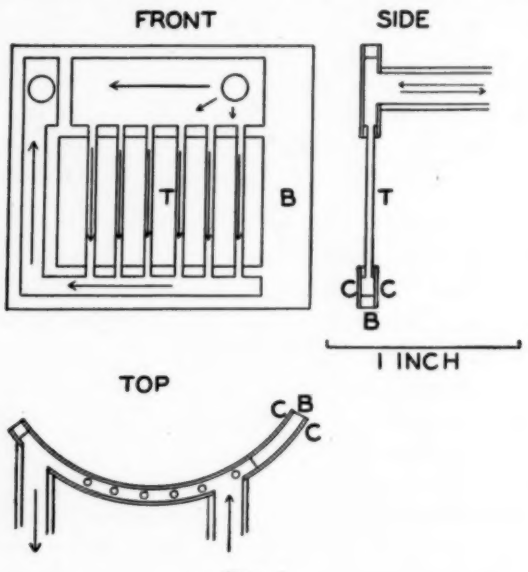

FIG. 4.

through the grid. Since the motor was found to become rather hot on continuous use, the arrangement shown schematically in Fig. 5 was finally adopted. Here A and B are two steel tanks of about 40 gallons in capacity, one of which is originally filled with distilled water. The glass tube T indicates the position of the water level in A. The tube C is connected to an air line, and

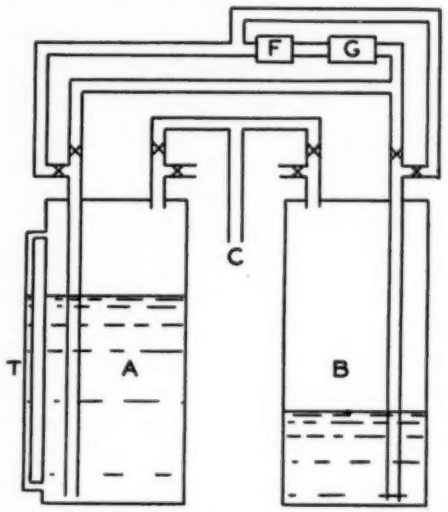

FIG. 5.

it is seen that by proper manipulation of the stopcocks X the water may be caused to pass back and forth from one tank to another through the grid G, being filtered each time by the filter F. The latter consists of a piece of tightly woven cotton cloth, with an area of about eight square inches. Water flow at a rate of about 25 gallons an hour was sufficient to prevent boiling in the grid tubes.

Details of the mounting of the filament are shown in Fig. 6. The filament itself consists of two strips of 0.001" platinum ribbon F. These strips are mounted between strips of copper C and nickel N pressed tightly together by flat-head screws as shown. Electrical current is conducted to the filament by the leads L. About 25 amperes were usually sufficient to bring the oxide coating to operating temperature. Mica strips were used for insulation.

The filament, grid, anode, and furnace were mounted on individual face plates, the vacuum seal being accomplished by the use of cylindrical rubber gaskets.

Figure 7 shows the electrical connections to the apparatus. The circuit was protected from overloading by a magnetic circuit-breaker B. This was found to be quite essential, for any

[9] K. W. Meissner and K. F. Luft, Ann d. Physik **28**, 667 (1937).

material increase in pressure in the chamber will cause arcing between the filament and grid, resulting in very high currents. The grid and anode voltages were supplied by a d.c. generator of 2-kw rating. A 1000-ohm resistance R_1 was

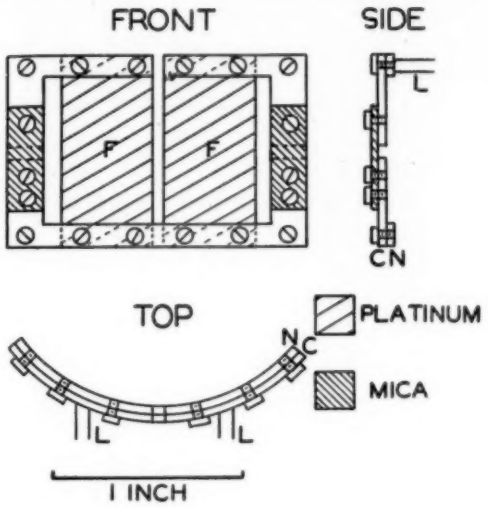

FIG. 6.

connected in series with the filament for stabilization of minor disturbances. The grid voltage may be changed relative to that of the anode by adjustment of the 900-ohm variable resistance R_2. Filament emission currents up to about 400 ma were obtained, approximately half being transmitted to the anode.

Measurement of pressure was performed with a Knudson gauge similar to that described by DuMond and Pickels.[10] This type of gauge is ideal for the present purpose, for it gives continuous readings, covers a wide range of pressures, and is extremely rigid. Its characteristics are, furthermore, not at all changed by the sudden bursts of pressure which occur because of evolution of gas from the furnace. The scale is linear at lower pressures, and nearly so at forepump pressures. Calibration was performed by using a McLeod gauge. A permanent horseshoe magnet was found to be quite sufficient for damping, and much handier than the electromagnet usually used.

The spectra obtained with this new atomic beam apparatus were practically free from a background present with earlier constructions and due to bands of gaseous impurities.

[10] J. W. M. DuMond and W. M. Pickels, Rev. Sci. Inst. 6, 362 (1935).

B. Spectral Apparatus

A Perot-Fabry interferometer was crossed with a prism spectrograph in making the measurements of hyperfine structure. The interferometer was placed between the collimator and the prism of the spectrograph. This is the arrangement for maximum intensity, as the entire areas of the interferometer plates are utilized in parallel light. The plates must, however, be very accurately plane and parallel when this method is used.

The spectrograph employed was a Steinheil, No. 5102, furnished with three glass prisms. The aperture of the lenses was 7.0 cm. In most of the work one prism furnished sufficient dispersion, and a focal length of 64 cm for both the collimator and the camera was used. While working in the infra-red, however, it was necessary to use a camera lens of 40-cm focal length in order to obtain sufficient intensity. In the investigation of the green triplet at 5180A, all three prisms were necessary to obtain sufficient dispersion.

The interferometer plates were made of fused quartz. They were 6.6 cm in diameter, and of slightly prismatic shape, the plane surfaces making an angle of about 30′ with each other.

These plates were coated with silver by sputtering in hydrogen. To ensure a uniform coating, a cathode area considerably larger than the area of the plates was employed, and the plate being sputtered was carefully centered with respect to the cathode. Pure hydrogen was obtained by using the palladium-tube method. The best surfaces were obtained by employing small sputtering currents and rather long sputtering periods. In a typical run, for example, a current of 9

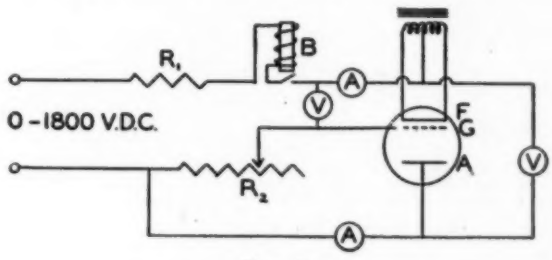

FIG. 7.

milliamperes maintained for 36 minutes produced a surface with a reflection coefficient of 0.90.

Measurements of the optical properties of the sputtered surfaces were made with a Weston photronic cell, and a wall-type galvanometer.

It was found possible to obtain surfaces for which the absorption coefficient ranged from 0.03 to about 0.06, depending on the density of the deposit used. Reflection coefficients of from 0.85 to 0.93 were employed.

The silvered surfaces of the interferometer plates were kept accurately parallel by spacers made of fused silica. The preparation of these spacers will now be described in some detail.

Opaque tubing of fused silica of 67-mm O.D. and 5-mm wall thickness was obtained from the Amersil Company, and was cut into the desired lengths with a high speed saw. Three small projections of clear fused quartz were then fused on each end, 120° apart, care being taken to have the corresponding projections of both ends accurately opposite one another. The projections were approximately hemispherical in shape, and about 3 mm in diameter. The next step was to grind the hemispheres on a flat surface of ground glass until the outer portions of their surfaces became plane circles about 2 mm in diameter. Carborundum was used for the initial rough grinding, and the finishing was accomplished using rouge.

After one set of the projections was finished, the other set had to be adjusted by careful grinding and polishing so that the planes formed by the two sets of surfaces became accurately parallel. The accomplishment of this task was very much simplified by using an interferometer, originally designed for plant physiological investigations by one of us.[11]

The interferometer housing consists of a brass cylinder which encloses the plates and spacer and is fitted with plate-springs of sheet steel for pressing the plates firmly against the spacer. This mounting, as well as the type of spring action, was adapted from the Perot-Fabry interferometer manufactured by Carl Zeiss, Jena. In order to secure absolutely reliable performance, however, it was necessary, especially for larger spacers, to provide both ends of the housing with adjusting springs. This design is similar to the one used by Meissner and Luft.[9] It may be mentioned that the original etalon of Perot and Fabry as constructed by Jobin,[12] also allowed adjustment of spring pressures from both ends.

After the interferometer is assembled, the spring pressures must be adjusted until the reflecting surfaces are accurately parallel to one another, as evidenced by the fact that the diameters of the interference rings formed by any small portion of the surfaces are exactly equal to those formed by any other portion. During the preliminary adjustment this condition is checked with the naked eye; a more accurate final adjustment is made with a telescope of small aperture but rather high magnifying power. A krypton discharge tube was used as light source for this adjustment. It was found that relatively small spring forces were required for this adjustment when the polishing was carefully performed in the manner described above. Another requirement for perfect adjustment is that the interferometer plates and the faces of the spacer projections be in optical contact. If these conditions are fulfilled a perfect adjustment can be retained for several days.

Because long exposure times were required, it was necessary to place the interferometer in a chamber that was maintained at constant temperature and constant pressure. For this purpose the chamber was equipped with a jacket through which water of constant temperature circulated. The temperature of this water was thermostatically controlled and was maintained constant to within 0.02°C. The interior of the chamber was easily reached by removing one end plate. This plate was fitted airtight to the chamber by the application of Apiezon stopcock grease. Plane parallel windows were sealed to the end plates of the chamber.

The spectra were recorded on Eastman plates; type 103 G was used for the visible region and type 1-P for the infra-red line 8806A. In the latter case the plates were hypersensitized with ammonia.

Most of the spectrograms were measured by means of an Abbe comparator (Zeiss, Jena, Model A, 1937), using magnifications ranging from six to twenty. In the case of two or three of the weakest lines, however, it was necessary to use even smaller magnifications in order to see the weak components of a line clearly. In these cases a Leiss comparator was used, set for a magnification of only three diameters. The possible

[11] K. W. Meissner, Physik. Zeits. **30**, 965 (1929); Jahrb. f. wiss. Botanik **76**, 208 (1932).
[12] Ch. Fabry and A. Perot, Ann. Chim. Phys. [7] **25**, 98 (1902).

error, of course, is increased by using such a small magnification.

II. RESULTS

A. General Features of the Lines

A large number of spectrograms were taken with interferometer spacings of 30.0, 41.7, and 60.0 mm. In agreement with the results of Meissner, it was found that whenever the hyperfine structure could be resolved, three nearly equally spaced components were present. The strongest component was always of longest wave-length, and the other two were always of nearly equal intensity.

The attribution of these components to the three isotopes of magnesium is undoubtedly justified, so in the following, we will refer to the wave numbers of the three components as ν_{24}, ν_{25}, and ν_{26}. In this investigation we have been primarily interested in the determination of the wave number differences of the various lines, given by $\Delta\nu=\nu_{26}-\nu_{24}$, and $\Delta'\nu=\nu_{25}-\nu_{24}$.

The $3\,^1P-m\,^1D$ series is very strongly developed in the atomic beam. Measurement of this series has been pushed to the member $m=11$. However, the satellites were extremely weak in the higher members, and starting with $m=7$, only one satellite could be observed. The accuracy of these measurements is naturally rather low.

Two members of the $3\,^1P-m\,^1S$ series appeared quite distinctly, and $\Delta\nu$ values were obtained in the case of the lines $m=5$ and $m=6$.

The intercombination resonance line

$$3\,^1S_0-3\,^3P_1,\ 4571\text{A},$$

appeared on a few plates, but was always too weak for the detection of any possible satellites.

In agreement with the results of previous investigations, no structure whatever could be detected in the case of the green triplet

$$5167\text{–}5184\text{A}\ (3\,^3P-4\,^3S).$$

B. Reduction of the Perot-Fabry Patterns

The quantitative evaluation of the wave number differences between the components of the lines was performed by applying Tolansky's method,[13,14] which is very convenient for close lines. This method is based on the fact that the squares of the diameters of the Perot-Fabry fringes form an arithmetical series of the first order and that the squared diameter values of the fringes of close lines show constant differences which are related to the wave number differences by a simple relation. The squares of the diameters of all the fringes measured on a compound line can be arranged in an array with horizontal and vertical rows with constant horizontal and vertical differences, from which the wave number differences can be found provided that the thickness of the spacer is known. In the case of the wave number difference between the Mg_{25} and Mg_{24} components, the relation is

$$\nu_{25}-\nu_{24}=\frac{(D_{25}^2-D_{24}^2)_{Av}}{(\Delta D^2)_{Av}}\cdot\frac{1}{2t}\ \text{cm}^{-1},$$

where $(\Delta D^2)_{Av}$ is the average value of the constant difference in D^2 between consecutive fringes of the same component, and where t is the thickness of the spacer in cm.

The value of $\nu_{26}-\nu_{24}$ is calculated in a similar manner.

C. Quantitative Results

Measurements were made on seventeen of the spectrograms taken. The values obtained from different plates agreed quite well among themselves, the mean error ranging from 0.0004 cm^{-1} for the stronger lines to about 0.005 cm^{-1} for the weakest ones.

The measured values of $\Delta\nu$ were found to fluctuate about definitely different values for different sizes of spacers. This is due to a slight "attraction" of strong spectral lines for neighboring weak ones, resulting in a "shrinking" of the observed separation.[15] The magnitude of this "attraction" depends on the distance between the two lines on the photographic plate which, in turn, depends upon the size of the spacer used. In such cases the most accurate results are obtained when the weak line being measured is (1) farthest from the neighboring strong line; or (2) midway between two strong lines. When the 60-mm spacer was used, condition (2) prevailed for the Mg^{25} components in the $3\,^1P-m\,^1D$ series, as the Mg^{26} component became super-

[13] S. Tolansky, J. Sci. Inst. **8**, 223 (1931).
[14] K. W. Meissner, J. Opt. Soc. Am. **31**, 405 (1941).
[15] O. Oldenberg, Ann. d. Physik **67**, 253 (1922).

TABLE I. Isotope shifts in Mg.

λ(A)	Transition	Mundie & Meissner	Meissner	Bacher & Sawyer
8806	$3\,^1P-3\,^1D$	0.0000 +0.0423±0.0004 +0.0851±0.0004	0.0000 +0.0412±0.0004 +0.0831±0.0004	0.0000 — +0.082
5528	$3\,^1P-4\,^1D$	0.0000 +0.0374±0.0004 +0.0709±0.004	0.0000 +0.0354±0.0004 +0.0714±0.0009	0.0000 — +0.065
4703	$3\,^1P-5\,^1D$	0.000 +0.038±0.001 +0.068±0.001	0.000 +0.034±0.002 +0.068±0.002	0.000 — +0.061
4351	$3\,^1P-6\,^1D$	0.000 +0.039±0.001 +0.070±0.001	0.000 — +0.061±0.003	— — —
4167	$3\,^1P-7\,^1D$	0.000 — +0.066±0.001	0.000 — +0.062±0.003	— — —
4057	$3\,^1P-8\,^1D$	0.000 — +0.067±0.003	Satellite present but not measurable	— — —
3986	$3\,^1P-9\,^1D$	0.000 — +0.067±0.003	— — —	— — —
3938	$3\,^1P-10\,^1D$	0.000 — +0.068±0.005	— — —	— — —
3904	$3\,^1P-11\,^1D$	0.000 — +0.069±0.005	— — —	— — —
5711	$3\,^1P-5\,^1S$	0.0000 +0.0266±0.0004 +0.0545±0.0004	0.0000 +0.0248±0.0015 +0.0543±0.0010	Asymmetry indicates structure similar to but narrower than that of 5528A
4730	$3\,^1P-6\,^1S$	0.0000 — +0.0625±0.0007	Line weak; no satellite visible	— — —

imposed on the Mg^{24} rings of next lower order number. Results obtained with the 60-mm spacer were therefore more heavily weighted in calculating the separations $\nu_{24}-\nu_{25}$ for this series.

Table I shows a complete list of measurements of $\Delta\nu$ and $\Delta'\nu$ made. For the sake of comparison, the results of Bacher and Sawyer and of Meissner have been included.

A fairly strong line at 4481A was found to be due to the Mg *II* transition ($3\,^2D-4\,^2F$); two components were found, with the intensity ratio of about 2 : 3. The splitting was calculated to be 1.000 ± 0.002 cm^{-1}.

III. DISCUSSION

It is seen from Table I that the observed isotope shifts are for the most part in substantial agreement with those of Meissner. The differences are in some cases larger than the combined predicted experimental errors, indicating that the true experimental error is somewhat larger than the quoted values. The latter are simply the average fluctuations of the values obtained among the different plates.

The measurement of the $3\,^1P-m\,^1D$ series has been carried to higher members. The values of $\Delta\nu(=\nu_{26}-\nu_{24})$ for the higher members of this series are found to fluctuate about an average value of 0.068 cm^{-1}. One would expect, therefore, that this value represents the (26–24) shift of the $3\,^1P$ term. This value is considerably higher than the approximate value of 0.056 cm^{-1} obtained by Meissner by extrapolation from the shift of the lower series members. Similarly, the values of $\Delta'\nu(=\nu_{25}-\nu_{24})$ seem to converge to a

value of 0.038 cm^{-1}, which may be taken as the (25–24) shift of the $3\,^1P$ term. It should perhaps be pointed out that the ground state of the singly ionized atom is considered as the level of zero energy for each isotope. Thus the shifts of the $3\,^1P$ term may be regarded as the corresponding shifts of the hypothetical "line" $(3\,^1P)_{MgI} - (3\,^2S)_{MgII}$ as has been done by Vinti.

Knowing the shift of the $3\,^1P$ term we can at once calculate the shifts of other terms involved in transitions with this term, in cases where the corresponding spectral lines have been resolved. Table II gives a list of term shifts obtained in this way. In this table

$$\Delta = T_{26} - T_{24} \quad \text{and} \quad \Delta' = T_{25} - T_{24}.$$

The analysis may be pushed further with the help of the very recent values of Fisher[6] for the shifts of the resonance line λ2852 $(3\,^1S_0 - 3\,^1P_1)$. For this line Fisher obtained values of +0.030 cm^{-1} and +0.053 cm^{-1} for $\Delta'\nu$ and $\Delta\nu$, respectively. The shifts of the $3\,^1S_0$ level are at once seen to be $\Delta' 3\,^1S_0 = 0.098$ cm^{-1} and $\Delta 3\,^1S_0 = 0.121$ cm^{-1}. Furthermore, if we accept Bacher and Sawyer's value, $\Delta\nu = +0.083$ cm^{-1}, for the intercombination line λ4571$(3\,^1S_0 - 3\,^3P_1)$, we obtain for the shift of the $3\,^3P_1$ level the value $\Delta 3\,^3P_1 = 0.038$ cm^{-1}. Finally, the sharpness of the lines $(3\,^3P_{0,1,2} - 4\,^3S_1)$ and $3\,^3P_{0,1,2} - 3\,^3D_{1,2,3})$ allow one to conclude that $\Delta 4\,^3S_1 \approx \Delta 3\,^3P_1$, and $\Delta 3\,^3D_{1,2,3} \approx \Delta 3\,^3P_1$.

In Table III a comparison is made of the theoretically predicted shifts of Vinti with the experimentally observed shifts of Meissner (M) and with those of the present investigation (MM). It is seen that the experimental results obtained in the present investigation are slightly further from the calculated values of Vinti than are the results of Meissner. The experimentally observed shift is in all cases about twice as large as the calculated value. The discrepancy between theory and experiment can be understood perhaps in view of the fact that the radial wave functions used are probably not very accurate.

Unfortunately, all of the other lines calculated by Vinti were found to be much too weak for resolution with the interferometer, and hence no check of the theory could be made from this direction.

It is interesting to note that the Mg^{26} satellite was measurable out to the member $m = 11$ of the $3\,^1P - m\,^1D$ series, while the Mg^{25} satellite could only be followed out to the member $m = 6$. A possible explanation is that the Mg^{25} line becomes "fused" with the base of the intense Mg^{24} line, although this explanation would not be valid in the case of larger plate separations.

The relative abundances of the isotopes Mg^{25}/Mg^{26} are found from the mass spectrograph to be 11.5/11.1. The difference in the abundances of these two isotopes should cause a corresponding difference in the intensities of the satellites in the spectral lines. A careful measurement of the intensities should therefore furnish a conclusive check on the order in which the satellites are assigned to the isotopes.

TABLE II. Calculated shifts.

Term	$\Delta'(cm^{-1})$	$\Delta(cm^{-1})$
$3\,^1P$	+0.038	+0.068
$3\,^1D$	−0.004	−0.017
$4\,^1D$	+0.001	−0.003
$5\,^1D$	0.000	0.000
$5\,^1S$	+0.011	+0.013
$6\,^1S$	—	+0.005

TABLE III. Comparison of calculated and observed shifts.

Transition	λ(A)	$\Delta\nu_{calc.}(cm^{-1})$	$\Delta\nu_M(cm^{-1})$	$\Delta\nu_{MM}(cm^{-1})$
$3\,^1P - 3s\,^2S$(MgII)		0.0264	0.056	0.068
$3\,^1P_1 - 3\,^1D_2$	8807	≦0.0434	0.0831	0.0851

This measurement was attempted in the present investigation. The line 8806A was chosen because this line exhibits the largest isotope shift. Furthermore, because of the high resolving power of the interferometer in this region, a very distinct separation of the components was achieved. Thus the instrumental conditions for the task were fulfilled. It was very soon found, however, that the photographic characteristics of the hypersensitized infra-red plates are not sufficiently constant for intensity measurements of the high accuracy required.

ACKNOWLEDGMENT

In conclusion we express our thanks to Dr. I. Walerstein for helpful discussions. Furthermore, the senior author wishes to acknowledge a grant in aid to research from the Rumford Fund of The American Academy of Arts and Science.

PHYSICAL REVIEW VOLUME 65, NUMBERS 9 AND 10 MAY 1 AND 15, 1944

On the Role of Polyatomic Gases in Fast Counters

S. A. KORFF AND R. D. PRESENT
New York University, New York, New York

(Received March 13, 1944)

The polyatomic gas serves a twofold purpose: (1) to quench ultraviolet photons and (2) to quench secondary emission by positive ions reaching the cathode. The characteristic property of a polyatomic molecule which is of importance for the operation of a fast counter is the large probability of predissociation from excited electronic states. The quenching of ultraviolet photons in the initial avalanche occurs through photo-decomposition of the polyatomic gas. In a fast counter containing a self-quenching mixture the polyatomic gas has invariably a lower ionization potential than the monatomic constituent. The positive ions make 10^5 collisions in crossing the counter and the electron transfer probability ensures that the positive ion sheath, when it reaches the cathode, is composed entirely of polyatomic ions. These are neutralized at about 10^{-7} cm from the wall and the excited neutral molecules predissociate in 10^{-13} sec. before they can liberate a secondary electron by an inelastic collision with the wall. With no supply of secondary electrons the discharge terminates. Other features of fast counter behavior are discussed and some of the conclusions reached have been checked experimentally.

INTRODUCTION

THE terms "fast" or "self-quenching" counter have been applied in recent years to that type of Geiger-Mueller counter in which the discharge terminates because of an internal process. These counters may be operated with comparatively low resistances and do not go into a continuous discharge except at high overvoltages. In order that a counter may operate as a fast counter, it must be filled with a certain minimum amount of polyatomic gas as a constituent. "Slow" or "non-self-quenching" counters, on the other hand, are filled with any monatomic or diatomic gas or mixture of such gases, and this type of counter goes into a continuous discharge unless operated with a high resistance or a vacuum-tube quenching circuit. Fast counters have been studied by Trost,[1] Ramsey,[2] Stever,[3] Korff,[4] and others. These investigations have dealt with the types of gas suitable for filling the counters, with measurements of the wire potential as a function of time, with measurements of dead time and recovery time, etc. A theory of the discharge mechanism in a slow counter has been given by Montgomery and Montgomery,[5] and their predictions are in good agreement with the observations of Ramsey, Trost, and others. The Montgomery theory has been extended to fast counters by Stever.[3] However, the role of the polyatomic gas in the discharge process has not as yet been explained. It will be shown here that the characteristic property of the polyatomic molecule which is important for the operation of a counter is the short lifetime of the excited electronic states against predissociation.

The excited electronic states of a diatomic molecule have sharp rotational levels well above the dissociation energy of the molecule, and predissociation is only an occasional phenomenon. In polyatomic molecules containing four or more atoms, predissociation is the rule rather than the exception, and the absorption spectrum in the ultraviolet shows diffuse absorption bands with the rotational structure obliterated, as well as regions of continuous absorption. This is essentially due to the opportunities for "crossing over" provided by the many intersections of the potential energy hypersurfaces extending over a wide range of energies. The heavier the molecule, the more diffuse is the spectrum and the more likely is predissociation. Light polyatomic molecules present an intermediate case, and the spectroscopy and photochemistry of each must be considered separately to determine the probable result of a given excitation.

It is to be noted that three distinct types of "quenching" are involved in the operation of a fast counter: (a) quenching of photons in the initial avalanche, (b) electrostatic quenching of the avalanche by the positive ion space charge,[5]

[1] A. Trost, Zeits. f. Physik **105**, 399 (1937).
[2] W. E. Ramsey, Phys. Rev. **57**, 1022 (1940).
[3] H. G. Stever, Phys. Rev. **61**, 38 (1942).
[4] S. A. Korff, Rev. Mod. Phys. **14**, 1 (1942).
[5] C. G. Montgomery and D. D. Montgomery, Phys. Rev. **57**, 1030 (1940).

and (c) quenching of the secondary emission when the positive ions reach the cathode. The quenching of the discharge involves both the electrostatic quenching and the quenching of secondary emission. We propose to discuss the role of the polyatomic gas in quenching cases (a) and (c).

PHOTON QUENCHING

First let us examine the role of the polyatomic gas in the initial avalanche. Common polyatomic constituents of counters are methane and alcohol vapor. Let us consider an argon-methane counter operating in the "proportional" region, in which the size of the pulse is proportional to the number of ions formed in the initial ionizing event. A theory of the formation of the avalanche in this case has been given by Rose and Korff.[6] Assuming that the electrons multiply by collision and that photoelectrons do not contribute to the cascade, they obtain a formula for the amplification or multiplication factor which agrees well with experiment as long as a sufficient amount of methane is present in the counter. When the relative or absolute amount of methane is reduced too far, the amplification factor is found to rise more steeply with increasing voltage than predicted by the formal, thus indicating an additional source of electrons. The dependence of this effect on the nature of the cathode surface led Rose and Korff to suggest that photoelectrons from the cathode were contributing to the avalanche. When the counter voltage was raised sufficiently, all the curves deviated from the formula. Rose and Korff point out that the inelastic collisions of electrons with methane molecules, leading to rotational and vibrational excitation, will dissipate the energy of the electrons and thus reduce the number of ultraviolet photons emitted in the avalanche. This cannot be the most important factor, however, in the quenching of the photons by the polyatomic gas since the greatest multiplication takes place in the high field region near the wire where the electrons gain enough energy in one free path to excite or ionize the argon atoms. Furthermore, a diatomic molecule should serve similarly, though less effectively, in dissipating the energy, and no amount of diatomic gas will quench the photon production. Rose and Korff have also suggested that collisions which cause electronic excitation of the polyatomic molecule will usually result in decomposition rather than in photon emission. This is in agreement with other evidence to be discussed below, and is supported by experiments of Glockler[7] in which electrons with 17-ev energy introduced into a methane-filled photo-cell produced no measurable photoelectric current. We wish to emphasize here that in a counter containing a mixture of gases the principal role of the polyatomic gas in the avalanche is to absorb the ultraviolet photons emitted by the inert gas (argon). Many photons originate in the avalanche from excited argon atoms. Ranging in energy from 11.5 to 15.7 ev, these photons would liberate electrons from the cathode (photoelectric threshold about 4 ev), were they not absorbed in the gas. Since a gas mixture containing fifty percent argon to fifty percent ether shows no evidence of cathode effect, according to Rose and Korff, it is evident that the argon photons are absorbed by ether molecules before they reach the cathode. This is also in accord with Ramsey's[8] double-counter experiment in which it was shown that when counter *A* discharged, if the photons from this discharge could reach the interior of counter *B*, then counter *B* discharged every time when the two were filled with a non-quenching gas (argon), and only at random times when the two were filled with a quenching gas (alcohol).

We inquire next into the details of the absorption act. When a molecule absorbs an ultraviolet photon and passes into an excited electronic state, there are several possible competitive modes of de-excitation: (1) decomposition (dissociation or predissociation), (2) radiation (fluorescence), and (3) deactivation by collision. Process (3) cannot occur in less than 10^{-8} sec., which is the collision time in an ordinary counter. Process (2) involves a radiation lifetime of 10^{-8} sec. Process (1), when possible, occurs within 10^{-11} to 10^{-13} sec. depending on the breadth of the levels. If the rotational structure is obliterated, the lifetime is about 100 times longer than if the vibrational structure is obliterated (continuous absorption). Diatomic molecules, in

[6] M. E. Rose and S. A. Korff, Phys. Rev. **59**, 850 (1941).

[7] G. Glockler, Proc. Nat. Acad. Sci. **11**, 74 (1925).

[8] W. E. Ramsey, Phys. Rev. **61**, 96 (1942).

general, as well as certain light polyatomic molecules possess stable electronic states with well-defined vibrational-rotational structure well above the dissociation limit or limits of the molecule. Excitation of the molecule into this region of energy results in re-emission of the absorbed photon or fluorescence and only rarely in dissociation. Hence, the photons produced in the discharge would not be quenched by a diatomic gas. On the other hand, if we examine the spectroscopic and photochemical data[9] for methane, ammonia, and other gases used in fast counters for which data are available, we can understand why these gases are photon-quenching. The photo-decomposition of methane in the ultraviolet is well known and the absorption spectrum, taken at a pressure of 1 mm of mercury, shows continuous absorption from 1450A down to at least 850A, the limit of observation. The ultraviolet photons emitted by excited argon atoms range from 1070A to 790A; hence, they are quenched by methane. Ammonia vapor also photodecomposes in the ultraviolet, and the spectrum shows continuous absorption below 1200A. Hence, ammonia also quenches the argon photons.

Evidence of the decomposition of the alcohol vapor in a fast counter has been obtained by Spatz;[10] the decomposition in the initial avalanche is to be attributed partly to electron impact and partly to photo-dissociation. As we shall see later, further decomposition occurs when the alcohol ions reach the cathode. The primary decomposition products are usually free radicals which combine to form a miscellaneous assortment of organic molecules. Some of these decomposition products will be quenching gases; however, with continued use of the counter all of the larger vapor molecules are broken up and the end products of the decomposition are a non-quenching gas, such as hydrogen or oxygen, and hydrocarbon goo deposited on the walls.[11] These considerations explain why fast counters go bad with continued use. Since about 10^{10} alcohol ions are decomposed at the cathode in each discharge, as will be explained in the next section, and since there are altogether about 10^{20} alcohol molecules in the counter, the counter will go bad after about 10^{10} counts. This is in accord with Spatz's observations. These considerations further explain why a methane counter has a shorter life than an alcohol counter. Methane is already far down the list of decomposition products of alcohol and itself can decompose only once or twice before it is reduced to a non-quenching mixture. We can also understand why argon must be mixed with a greater proportion of methane than of alcohol to produce a photon-quenched counter, i.e., a counter with no cathode effect. This is due partly to the greater number of vibration-rotation levels available for inelastic electron impacts in the case of the alcohol counter and partly to the higher quantum yield of the photo-decomposition of alcohol.

Some of the results of Wilkening and Kanne[12] on localization of the discharge will be examined next. The discharge in the Geiger region normally spreads the entire length of the wire in both slow and fast counters.[3] A reduction in the field near the central wire by some artificial means, or the presence of an obstacle such as an insulating bead, will interrupt the spread of the discharge in a fast counter but not in a slow counter. In the latter case, photoelectrons from the cathode spread the discharge beyond the obstacle. Wilkening and Kanne used various devices to interrupt the spread of the discharge and measured the effectiveness of the localizing devices in various gases. Fast counters showed 100 percent "localization." However, a mixture of 1 cm of methane with 9 cm of argon showed only a 50 percent localization. This is clearly due to the fact that the photon-quenching is incomplete in this case, as we may verify from the amplification factor curves given by Rose and Korff; at 10-cm pressure even a 50 percent argon-methane mixture shows evidence of appreciable photo-effect. Counters filled with monatomic and diatomic gases showed "zero localization," or complete spread of the discharge, corresponding to the total absence of photon-quenching. There should exist a close correlation between the

[9] Cf. Rollefson and Burton, *Photochemistry* (Prentice-Hall, New York, 1939). Data on the absorption spectrum in the ultraviolet of many polyatomic molecules may be found in tables at the end of the review article by H. Sponer and E. Teller, Rev. Mod. Phys. **13**, 75 (1941).

[10] W. D. B. Spatz, Phys. Rev. **64**, 236 (1943).

[11] L. M. Yaddanapalli, J. Phys. Chem. **10**, 249 (1942).

[12] M. H. Wilkening and W. R. Kanne, Phys. Rev. **62**, 534 (1942).

extent of localization and the length of the proportional region. It is well known that fast counters have a much longer proportional region than slow counters at the same total pressure. This is due to the more rapid rise of the amplification factor of a slow counter with increasing voltage, which is in turn due to the photoelectric effect at the cathode. Thus, the spreading of the discharge beyond an obstacle and the rapid rise of the amplification factor are due to the same cause: photons in the avalanche. The counters found by Wilkening and Kanne to show 100 percent localization are all counters containing heavy polyatomic vapors which are present in sufficient amount to absorb out the argon photons. The methane-argon counter showing 50 percent localization has a short proportional region, as may be inferred from Fig. 2 of reference 6. Counters filled with diatomic gases go over directly into a continuous discharge without any observable proportional counting, and show zero localization.

Finally, we mention a further consequence of the photon-quenching, which has already been pointed out by Weisz[13] and which is of minor importance for most counters. In a slow counter, some of the photoelectrons produced at the cathode will attach themselves to neutral molecules to form negative ions which drift in toward the central wire. In the high field near the central wire the electron will detach itself and start another avalanche unless the potential across the counter is below the starting potential at this time. Since the probability of electron attachment is very small for most counter gases, this effect will be unimportant except in the case of oxygen, where one collision in 10^4 leads to attachment. Since the photoelectrons make about 10^4 collisions in traversing the counter, negative molecular ions O_2^- will play a role in the discharge.

SECONDARY EMISSION QUENCHING

We consider next the transition from the proportional region to the Geiger region in which the size of the pulse is independent of the number of ions formed in the initial ionizing event. At the threshold voltage of the Geiger region, the amplification factor theoretically rises to infinity; in practice the Geiger threshold corresponds to an amplification factor between 10^8 and 10^{12}. Let us assume that the counter has a negligible resistance in series with it. Then when the Geiger threshold is reached, a slow counter will go into a "continuous" discharge, whereas a fast counter will give a single sharp pulse. Because of the absence of resistance, the counter is at operating potential during the entire time that the positive ions are moving out to the cathode. The electric field intensity in the vicinity of the wire is below the threshold field until the ions have moved out to the "critical distance." [3] The positive ions then have drift velocities of the order of one-tenth their thermal velocities and the kinetic energy they acquire between collisions is less than 0.1 ev. Thus, they can neither excite nor ionize, so that if no further ionizing particles enter the counter, nothing happens until the ions reach the cathode and are neutralized. It is at this juncture that the behavior of an argon-filled counter differs from that of a methane-filled counter. Secondary emission takes place in the argon counter and, since the counter is at operating potential at this time, the entire cycle is repeated. Thus the discharge in a slow counter is self-perpetuating although the avalanches are intermittent. In a methane counter, on the other hand, the discharge is terminated when the methane ions are neutralized, and no secondary emission can occur. The explanation of this is to be found in the decomposition of the neutralized methane.

Details of the neutralization act and subsequent secondary emission will be considered next. When an argon ion approaches to within 10^{-7} cm of the cathode surface, the field of the ion becomes great enough to extract an electron from the metal. An electron near the top of the Fermi distribution may penetrate the barrier separating the potential well of the metal from the potential well of the ion. The neutralized atom is formed in an excited state, the energy of excitation being close to $I-\phi$, where I is the ionization energy of the atom and ϕ the work function of the metal (in the case of argon ions and a copper cathode, the neutralized atoms are formed in the excited state at 11.5 ev). The critical distance of approach at which the probability of neutralization approaches unity,

[13] P. Weisz, Phys. Rev. **62**, 477 (1942).

has been calculated by Oliphant and Moon,[14,15] using the Fowler-Nordheim formula. The probability of neutralization is an extremely sensitive function of the distance and for ions of thermal velocities approaching a copper surface the critical distance is about 5×10^{-8} cm. Thus, neutralization must take place before the ions are 5×10^{-8} cm from the wall, and the neutralized atoms should reach the wall in about 2×10^{-12} sec. Many atoms, however, do not reach the wall since the momentum communicated to the ion on neutralization is of the same order of magnitude as its initial thermal momentum. It has been found experimentally that He^+ ions which collide with an outgassed platinum surface at a glancing angle escape largely as neutral atoms in the metastable state. This indicates that an ion may be neutralized without making an inelastic collision with the wall. Many neutralized atoms, however, will approach the surface close enough to transfer their excitation energy to an electron in the metal, resulting in the emission of a secondary electron if $I>2\phi$. The probability of secondary emission by an excited atom approaching the surface has been calculated by Massey;[16] according to Massey's formula an atom of thermal velocity must approach to within 2×10^{-8} cm of the surface to make secondary emission probable, i.e., the wave functions of the atomic and metallic electrons must overlap. Since the radiation lifetime of the excited state of argon formed on neutralization is 10^{-7} sec., many of the argon atoms will liberate electrons from the cathode.

Let us now consider what happens when a methane ion captures an electron from the wall. The ionization energy of methane is 14.5 ev and the molecule resulting from the recombination has therefore the same excitation as a molecule that has absorbed light of wave-length 1200A. The spectrum of methane, as has been previously mentioned, shows continuous absorption below 1450A, indicating a lifetime against decomposition of the order of 10^{-13} sec. for the excited molecule. If this figure were exact and if the molecule required 2×10^{-12} sec. after neutralization to reach the wall, only about one molecule in 10^9 could reach the wall before decomposing. We can suppose that the electrostatic image force orients the approaching polyatomic ion so that the charged end faces the surface; thus, neutralization occurs when the front end of the ion is 5×10^{-8} cm from the surface and about the same time is required to reach the surface as for the neutralized atom. Even after the polyatomic molecule comes into contact with the surface, i.e., within range of the van der Waals forces, a transfer of electronic excitation energy from the chemical bond in which it was originally localized, across several other bonds to an electron in the metal, is still less likely than a decomposition. The secondary emission is therefore very small. We must also note that a radiation lifetime of 10^{-7} sec. implies that one molecule per 10^6 will radiate instead of decomposing. Since the photoelectric yield for the cathode surfaces used is of the order of 10^{-4} electrons per quantum, the secondary emission from this source amounts to one electron per 10^{10} incident positive ions. We take this figure to represent the total secondary emission.[17]

The average number of ions formed in a fast counter avalanche at the beginning of the Geiger region is about 10^9. Hence, we can understand why the secondary emission is quenched and a single sharp pulse obtained from a counter filled with methane. In order to determine whether a given gas by itself will make a fast counter, we have to investigate its absorption spectrum at wave-lengths corresponding to an excitation energy of $I-\phi$. If the absorption spectrum is diffuse or continuous, corresponding to decomposition in this region, then the gas will make a fast counter. To take another example: The ionization energy of ethyl alcohol is 11.3 ev and the neutralized molecule is formed about 1700A above the ground state. The spectrum of the vapor shows continuous absorption below 2000A, and this is accompanied by photo-decomposition. The quantum yield of the photo-decomposition is of the order of unity. Hence, we should expect alcohol vapor to make a good fast counter. A diatomic molecule generally possesses discrete

[14] M. L. E. Oliphant and P. B. Moon, Proc. Roy. Soc. **A127**, 388 (1930).
[15] M. L. E. Oliphant, Proc. Roy. Soc. **A124**, 228 (1929).
[16] H. S. W. Massey, Proc. Camb. Phil. Soc. **26**, 386 (1930).

[17] Recombination of secondary electrons with incoming positive ions will further reduce the chance of producing a new avalanche.

states between the dissociation energy and the ionization energy; thus, on neutralization a diatomic molecule will not decompose. This explains why counters filled with diatomic gases show slow counter action. Since a heavy organic molecule has a large probability of predissociating at all energies so that the ultraviolet absorption spectrum is everywhere diffuse or continuous, such a gas will invariably make a fast counter. The triatomic gases must be considered separately. The absorption spectra of H_2O, CO_2, N_2O, SO_2, H_2S, and CS_2 show bands with diffuse rotational structure converging on the ionization energy of the molecule as a limit. The broadening of the levels would correspond to a lifetime of the order of 100 times that of a heavy molecule, hence secondary emission would be much more probable. Some experiments we have performed with counters filled with the above-mentioned triatomic gases (connected to low resistances) gave no evidence of a Geiger region.

A further consequence of the mechanism of secondary emission quenching outlined above is that the frequency and multiplicity of multiple pulses should increase slowly along the plateau of a fast counter. The numerical estimates of secondary emission given above would lead one to expect about one double pulse in ten or one triple pulse in one hundred at the beginning of the Geiger region. This is roughly in agreement with what one observes on the oscilloscope screen. As the voltage across the counter is raised, the charge collected per count is found to vary linearly with the over-voltage and measurements along part of the plateau show that the charge increases by a factor of more than ten (see Appendix). An increase in the number of ions reaching the cathode results in an increased secondary emission and a corresponding increase in the frequency and multiplicity of multiple pulses. From the numerical estimates given above one would expect that toward the end of the plateau several secondary electrons on the average would be emitted when the positive ion sheath reached the cylinder. Under these circumstances practically every pulse would be a multiple of large multiplicity; in fact, the oscilloscope shows sprays of multiple pulses toward the end of the Geiger region. If electronic circuits of high resolving power for fast counting are used with the counter, these multiple pulses will give rise to many spurious counts. The slope of the counting-rate plateau is thus to be attributed to the increasing frequency and multiplicity of the multiple pulses leading to an increasing number of spurious counts; and the Geiger region terminates when the secondary emission becomes great enough to make the discharge self-sustaining. In order to make the plateau as flat and long as possible, the secondary emission must be small, and this implies that the polyatomic molecules used should have a short lifetime against dissociation and the photoelectric efficiency of the cathode material should be low. It has been found empirically that fast counter action is improved by a treatment of the cathode surface which reduces the photoelectric efficiency, e.g., the NO_2 treatment of copper.[3] It has been suggested that the factor which actually limits the width of the plateau is the occurrence of spurious counts due to "a sensitive condition of the surface of the cathode from which are emitted electrons when an electric field is present." [5] The fields at the cathode or even at the anode (10^4 v/cm) are not great enough to produce field emission for which a field of about 10^7 v/cm is required. Unless the metallic surfaces are rough or the central wire has become pitted, this effect will be unimportant compared with the spurious counts arising from multiple pulses.

So far the discussion has been restricted to fast counters containing a pure polyatomic gas. If we consider next a self-quenching counter which contains a mixture of a quenching and a non-quenching gas, the question arises how the secondary emission is suppressed. Since a counter containing 90 percent argon to 10 percent alcohol is self-quenching, it is necessary to explain why no argon ions reach the cathode when there is a small amount of alcohol present. The explanation depends on the relative size of the ionization potentials of the two gases: 11.3 volts for C_2H_5OH and 15.7 volts for argon. In the first place, the positive space charge formed in the initial avalanche must have a greater proportion of alchol ions than would be expected from the relative concentrations. This is partly due to the fact that the avalanche electrons can ionize alcohol molecules before they have acquired enough energy to ionize argon atoms, and

the ionization cross sections are proportional to the excess energy of the electron above the ionization energy. Also, the ionization efficiency in C_2H_5OH probably exceeds that in argon because of the greater number of electrons per molecule. However, the energies of the electrons are in all cases sufficient to produce a number of argon ions comparable to the number of alcohol ions. The reason why a negligible number of argon ions reaches the cathode is that electron transfer takes place during the passage of the ion sheath across the counter. During this time the argon ions make about 10^5 collisions with alcohol molecules, and since the ionization energy of the argon atom is greater than the ionization energy of the alcohol molecule, an electron can be transferred from the molecule to the ion. The transfer of an electron from an argon atom to an alcohol ion is energetically impossible because the kinetic energies are only about 0.1 ev. This process is accompanied by the emission of a photon of 4.4 ev (difference of the ionization energies) which is quenched by the alcohol vapor. This effect has been investigated by Kallmann and Rosen,[18] who found that the cross section for electron transfer is of the order of magnitude of the gas kinetic cross section in the case of an ion beam moving through a gas of the same species. In the case of an ion beam moving through a gas of a different ionization potential, the cross section is somewhat less, but no appreciable number of argon ions can reach the cathode after 10^5 collisions. In the commonly used self-quenching counters containing a mixture of gases, the ionization potential of the polyatomic constituent is invariably less than that of the inert gas. If the situation could be reversed, so that the inert gas has the lower ionization potential, then electron transfer would take place in the reverse direction and no polyatomic ions would reach the cathode. In such a counter photons would be quenched but not the secondary emission. The experimental tests to be described in the next section bear this out.

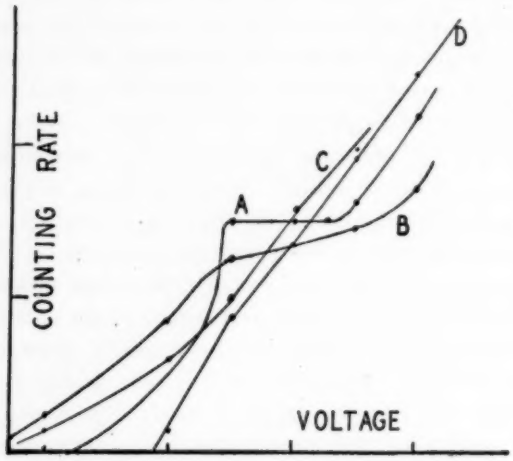

FIG. 1. Effect on plateau of methane counter produced by adding xenon. Curve *A*, pure methane; curve *B*, 0.3 mm of Xe added; curve *C*, 1.5 mm of Xe added; curve *D*, 1.5 cm of Xe added. Xenon has a lower ionization potential than methane, and consequently some xenon ions reach the cylinder where they produce secondary electrons and hence spurious counts. Methane pressure, 5 cm.

EXPERIMENTAL TESTS

We have made some tests on counters containing methane with varying small amounts of a non-quenching gas of lower ionization potential. The gases used were xenon, air (O_2), and water vapor. The resistances used were $\frac{1}{4}$ megohm and other values down to 1000 ohms. With such low resistances a counter containing a pure non-quenching gas goes directly into a self-sustaining discharge with no Geiger region and without any appreciable region of proportional counting. A 9-cm CH_4+1-cm Xe counter, on the other hand, has a well-defined proportional region, as one would expect from the quenching of photons by the methane vapor. Figure 1 shows the counting rate *vs.* voltage curves for various mixtures of CH_4 and Xe. It is seen that the addition of 1.5 mm Xe to a CH_4 counter completely effaces the plateau. The oscilloscope shows that in place of a Geiger region there is a short voltage range between the proportional region and the self-sustaining discharge in which nearly every pulse is a multiple. From Fig. 1 we see that 0.3 mm of Xe is sufficient to alter the plateau substantially. This indicates that the presence of Xe (ionization potential 12.1 v) to one part in a thousand causes the production of an observable amount of secondary emission, manifested by multiple pulses and the resulting spurious counts which tilt the plateau. On the other hand, addition of 1.5 cm of argon whose ionization potential is 15.6 v (see Fig. 2) did not alter the flatness of

[18] Kallman and Rosen, Zeits. f. Physik **61**, 61 (1930).

the plateau. Similar results were found for the methane-water vapor (Fig. 2) and methane-air (Fig. 3) mixtures, thus confirming the mechanism discussed previously. It is interesting to note that mercury vapor, which has a vapor pressure of 10^{-3} mm at room temperature, contaminates most counters to about one part in 10^5 without affecting the plateau. Mercury has an ionization potential (10.4 v) less than that of methane (14.5 v). A methane counter containing a drop of mercury was totally immersed in a hot water bath, and it was observed that when the temperature rose to 82°C (vapor pressure of mercury 0.1 mm), the normal self-quenching action was destroyed. The tests on the triatomic gases, which showed no plateau when used with a $\frac{1}{4}$-megohm resistance, have been discussed in the previous section.

In all the experiments the counter used was 1.2 cm in diameter and 10 cm long, and had a 3-mil tungsten central wire. The counter was removed from the system, washed with acid, replaced, and baked under vacuum, and the wire

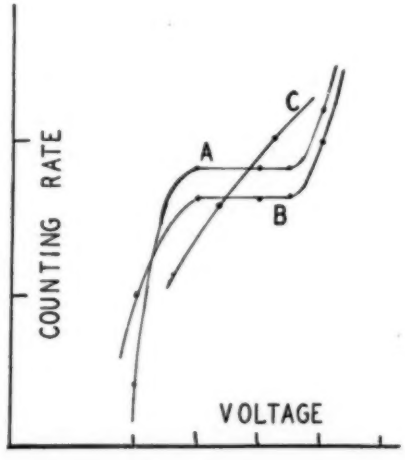

FIG. 2. Effect on plateau of methane counter produced by adding argon or water vapor. Curve *A*, pure methane; curve *B*, 1.5 cm argon added; curve *C*, 1.5 cm water vapor added. Note that the argon does not influence the flatness of the plateau while the addition of water vapor causes the plateau to disappear. The ionization potential of argon is greater than that of methane, while that of water vapor is less.

was glowed between tests. The counting rates were observed with a 10-microgram radium source 12-cm distant, and were recorded on a scale of 64 counter. Each point on each curve represents between 2000 and 10,000 counts. The counting rate seldom exceeded 100 per second and was usually about 30 per second. It was therefore well within the resolving time of the counter. The voltages used ranged between 1000 and 1500. Neither the counting rates nor the

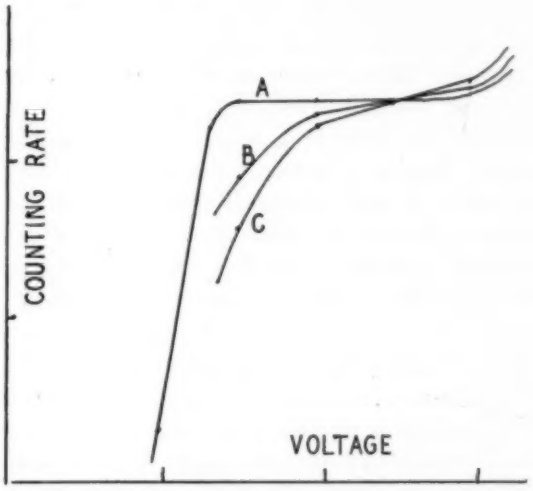

FIG. 3. Effect on plateau produced by adding air to a methane counter. Curve *A*, pure methane; curve *B*, 1.5 mm air added; curve *C*, 6 mm of air added. Methane pressure, 5 cm.

voltages are numerically indicated in the figures since the quantities depend on the position of the radium source and the size of the counter and gas pressure, and hence their magnitude is not significant. For example, curves *A* and *B* in Fig. 2 have been separated to allow the plateaus to be inspected. Such a shift can be accomplished either by moving the source slightly or by shifting ordinates. The plateaus normally observed were about 50 volts long. A resistance of 250,000 ohms was used in all cases.

APPENDIX: LINEAR VARIATION OF CHARGE WITH OVER-VOLTAGE

Stever[3] and Simpson[19] have found that the charge collected per count in a fast counter varies linearly with over-voltage except for high over-voltages. At the threshold of counting (starting potential), which we shall assume to be close to the threshold of the Geiger region, the most intense ionization of the avalanche occurs in the immediate vicinity of the wire where the field is

[19] We are obliged to Dr. John A. Simpson for communicating to us some of his unpublished work.

about 10^5 v/cm. Since the mean free path is 10^{-4} cm in a counter at 10-cm pressure, an electron near the wire can gain enough energy from the field between successive collisions to ionize. Let E_c denote the critical field for intense ionization which is reached in the neighborhood of the wire (radius r_w) when the voltage is raised to the starting potential V_s. As the operating voltage V is raised above V_s, the critical field moves out from the central wire, and if r_c denotes the radius of the critical field and c the capacitance per unit length of the counter, then $E_c=2cV/r_c=2cV_s/r_w$. It follows that r_c-r_w is proportional to the over-voltage. Now the total number of electrons produced in the region of intense ionization is readily seen to be proportional to $\exp \int_{r_w}^{r_c} K(r)dr$, where $K(r)$ denotes the average number of electrons produced by ionization when one electron moves through unit distance. $K(r)$ is proportional to the ionization cross section which depends on the electron energy, which in turn depends on r. However, the energy loss through inelastic collisions is so great that the electron energy increases only slowly with decreasing r. For the electron energies attained in the region of intense ionization, the ionization cross section varies linearly with energy at first and then increases more slowly. Hence we may neglect the variation of $K(r)$ in the small interval over which the integral is evaluated. The charge collected per count is thus proportional to $\exp\{(r_c-r_w)/\bar{\lambda}_i\}$ where $\bar{\lambda}_i=1/\bar{K}=$averaged mean free path for ionization. For the counters used $\bar{\lambda}_i\sim10^{-2}$ cm and $r_c-r_w\lesssim10^{-3}$ cm for not too high over-voltages. On expanding the exponential and neglecting powers of $(r_c-r_w)/\bar{\lambda}_i$ greater than the first, we obtain a linear dependence of the charge collected on r_c-r_w and thus on $V-V_s$ which is the over-voltage. The more rapid rise of the charge collected at high over-voltages is essentially due to the sprays of multiple pulses. Toward the end of the Geiger region, an initial ionizing event will frequently produce a multiple instead of a single pulse. The charge collected increases with the frequency and multiplicity of the multiple pulses.

The Effect of Intense Electrostatic Fields on the Reflectivity of Tungsten

CHARLES KENNEDY STROBEL
Department of Physics, University of Pittsburgh, Pittsburgh, Pennsylvania
(Received September 17, 1943)

The results of a study of the effects of intense electrostatic fields on the reflectivity of tungsten show no detectable change with surface voltage gradients up to about 6×10^8 volts/cm. The indications are that, in order to produce observable effects on the reflectivity of tungsten, it will probably be necessary to use much higher surface voltage gradients and a more sensitive detecting means.

I. INTRODUCTION

IN a survey prior to the present investigation, no reference to the effect of intense electric fields on the reflectivity of metals was found. However, references were found dealing with the effects of such fields on the vaporization and resistance of metals.

Worthing,[1] working with tungsten at incandescence, observed a decrease in the vaporization rate and resistance with surface voltage gradients of about 10^6 volts/cm. In similar studies with molybdenum, Estabrook[2] observed a decrease in vaporization rate and an increase in resistance. In the case of metals, in accord with theories of surface potential barriers, and as suggested by Hutchisson,[3] one might expect not only modifications of vaporization rates and resistivity, but also a modification of the reflectivity. The purpose of the present research was to investigate whether or not any such changes of reflectivity for tungsten are obtainable.

II. APPARATUS

The apparatus consisted of a high voltage d.c. power supply, a vacuum test chamber, a mount for the test sample, a high vacuum pumping system, and pyrometer measuring devices. Except for the pyrometer equipment, all was enclosed in wire screen cages.

In the high voltage d.c. power supply the 60,000-volt secondary of a 3-kva transformer was connected through a Kenotron rectifier and safety devices to a filter circuit, consisting of a parallel arrangement of condenser and resistance, designed to reduce the a.c. ripple to less than 0.5 percent. Part of the resistance of the filter circuit was that of a high voltage voltmeter, to whose terminals the d.c. power supply line was connected.

The voltmeter consisted of a high quality 1582-megohm resistor[4] connected in series with a shunted mirror galvanometer. Except for a small opening at the front, the galvanometer was enclosed in a grounded metal case.

The vacuum test chamber is shown in Fig. 1. It was a vertical glass tube about 20 in. long by $2\frac{7}{8}$-in. O.D., having four sealed electrical terminals and an annular indentation near the bottom for supporting the mount for the test sample. The bottom of the tube was connected to the pump. The top edge was ground smooth for sealing.

The test sample was a fine filament of tungsten wire,[5] which was mounted vertically along the axis of a spaced turn, single layer, helical coil of Kovar wire called the "potential coil." This arrangement makes possible pyrometer studies of the test sample while its surface is subjected to intense electrostatic fields. The voltage gradient at the surface of the test filament is given by

$$G=\frac{E_{AB}}{R_B \ln \frac{R_A}{R_B}},$$

where R_B = radius of tungsten filament; R_A = radius of helical or "potential coil"; E_{AB} = potential difference between "potential coil" and filament.

[1] A. G. Worthing, Phys. Rev. **17**, 418–420 (1921).
[2] G. B. Estabrook, Ph.D. Thesis, University of Pittsburgh (1932); and Phys. Rev. **63**, 352–358 (1943).
[3] E. Hutchisson, Phys. Rev. **47**, 328 (1935).
[4] International Resistance Company, Type MVO 1500-megohm resistor.
[5] Supplied by the General Electric Company, Lamp Development Division.

Very high gradients are obtainable with moderate applied voltages when the test filament has a very small diameter. The radius of the "potential coil" is relatively unimportant. This radius was made rather large, however, in order to minimize the sidewise electrostatic forces resulting from lack of centering.

The diameter of the tungsten filament was about 0.000875 cm. Its length was 13.5 cm. The "potential coil" was a 16-turn coil of 0.153-cm diameter wire, having an over-all length of 7.7 cm and a mean diameter of 4 cm.

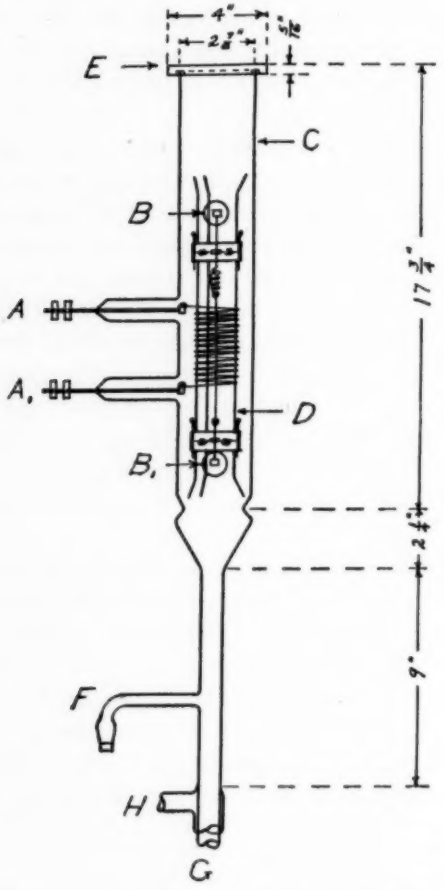

FIG. 1. Glass vacuum chamber C and mount D for potential coil and test filament. A–A_1, lead-in terminals for potential coil; B–B_1, lead-in terminals for test filament; E, brass top plate; F, tube leading to ionization gauge; G and H, leads to mercury trap and pumps.

As Fig. 1 shows, the mount consisted of three vertical glass rods with extensions bent outward for support purposes, spaced equally about the "potential coil," and fused to two cylindrical glass collars. Each collar supported a small brass centering disk in a horizontal position by means of four radial springs. The outer end of each spring was looped through a hole in the wall of the glass collar. By means of tapered glass pins through these loops, the brass disks were centered. The test filament was attached to the centering disks and was held taut by means of a strong Kovar spring. The terminals of the "potential coil" and filament were connected to the four sealed-in terminals A, A_1, B, and B_1.

The high vacuum pumping system was of the usual type with provision for flushing the system with dry air.

Three different optical arrangements were used for the pyrometer measurements.

In the first arrangement, a 100-watt light source, focused on a small celluloid diffusing screen attached to the outside wall of the vacuum chamber, served to illuminate the test filament. Reflected light from the tungsten test filament passed between the center turns of the "potential coil" and an achromatic lens to a standard optical pyrometer. The orientation was such that no light reflected from the glass walls could enter.

The pyrometer, of the disappearing filament type, was equipped with a red glass filter and extra lenses. The image of the tungsten test filament in the focal plane was of about the same size as the pyrometer filament. The pyrometer was calibrated in the usual manner.

The second arrangement was similar to the first, except that two 100-watt light sources were used, one to illuminate each side of the test filament.

In the third arrangement, shown in Fig. 2, the double light source as described was used with an alternate type of pyrometer. The tungsten test filament itself was used as a pyrometer filament. A ribbon filament lamp, introduced back of the test chamber, served as the background source. The light from both the background, kept at a constant brightness, and the tungsten test filament were viewed through a Ramsden eyepiece and red filter glass. A pyrometer balance was obtained by varying the voltage applied to the light sources illuminating the test filament. One of the two lamps of the double light source was calibrated against a standard lamp on a photometer bench, with the eyepiece and filter used in the tests.

III. METHODS AND DATA

With a tungsten test filament in position, in a high vacuum, better than 10^{-6} mm Hg in all cases, various d.c. voltages up to 36 kilovolts were applied between the filament and the concentric "potential coil," and corresponding test filament brightness measurements were made. The filament was made a positive grounded electrode in order to eliminate electronic discharge.

Six pyrometer tests were made under various conditions. In all tests, the d.c. potential difference between the "potential coil" and filament was varied from zero to the highest value possible without filament vibration, in approximately equal voltage steps. At each step, five or six pyrometer balances were made. Some tests were made with increasing pyrometer filament brightness, others with decreasing filament brightness.

In the first test, the first optical arrangement described under apparatus was used with the light source connected to a 115-volt a.c. power supply. A 750-megohm damping resistor was connected in the high voltage d.c. supply line, to limit vibration of the test filament.

In the second test, the first optical arrangement was used, but the light source was connected to a constant voltage d.c. supply and no damping resistor was used.

Because of the uncertainty of the d.c. voltage drop across a damping resistor in the high voltage d.c. supply line, the high probability of filament breakage when no damping resistance was used, and the non-uniform illumination of the filament by a single light source, the arrangements for the remaining tests were modified.

In the third test, the second optical arrangement was used with the double light source supplied by a constant d.c. voltage. A 360-megohm damping resistor was so connected in the high voltage filter circuit as to permit direct measurement of the potential difference between the test filament and potential coil and also limit the vibration of the test filament.

In the fourth, fifth, and sixth tests, the third optical arrangement as shown in Fig. 2 was used with the double light source supplied with a constant d.c. voltage. Preliminary tests were made with the optical system to determine conditions of high sensitivity and accuracy as described by Worthing and Forsythe.[6] The 360-megohm damping resistor was connected as in the third test.

During the sixth test, the vacuum chamber was irradiated by radium in an attempt to eliminate charges on the glass surfaces. There was no observable effect on the results obtained.

Certain data and computed values obtained for these tests are tabulated in Tables I and II. Table I shows a sample set of data for an individual test. Table II shows a summary of pertinent data for all six tests.

IV. DISCUSSION

The summary of Table I shows that, in all tests, any change in the average brightness or reflectivity of the filament due to a change in voltage gradient was much less than the range of measured brightness or reflectivity in obtaining a set of pyrometer measurements. With the most sensitive arrangement tried, there was no certain change in brightness or reflectivity of the tungsten filament, within the range of surface voltage gradients used.

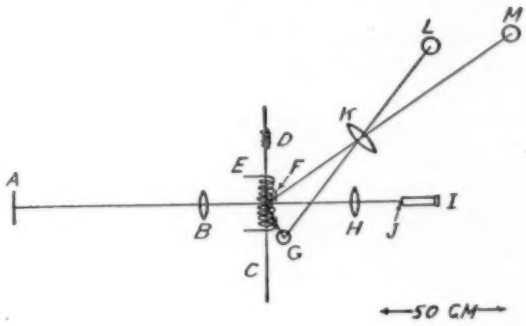

FIG. 2. Optical arrangement using test filament as pyrometer filament. *A*, ribbon filament background lamp; *B*, camera lens; *C*, tungsten test filament, kept taut by spring *D*; *E*, potential coil; *F*, diffusing screens on vacuum chamber wall; *G*, mirror; *H* and *I*, parts comprising the eyepiece of a disappearing filament optical pyrometer with an adjustable aperture at *J*; *K*, lens for concentrating light from sources *L* and *M* on the test filament at the axis.

A comparison of the results for the six tests seems to indicate that the results of the third and sixth tests are most reliable and that we may use them to indicate the maximum change

[6] A. G. Worthing and W. E. Forsythe, Phys. Rev. 4, 163–176 (1914).

in reflectivity which might have occurred and still have been undetected. Thus, the results of Table I indicate that the average brightness or relative reflectivity of the tungsten filament could not have changed by more than about 3 percent when the surface gradient was varied from 0 to 6.48×10^8 volts/cm.

In order to proceed further with this study, it seems that it would be necessary either to obtain a more sensitive means of measuring reflectivity or to obtain higher surface voltage gradients.

In the present work the sensitivities of the two pyrometer arrangements were limited by the smallness of the test filament, and the surface voltage gradient was limited by filament vibration, which was apparently initiated by mechanical shock or electrical disturbances in the system.

There are various theories of metallic reflection which indicate that an electric field should affect the reflectivity. Schiff and Thomas[7] present a quantum theory of metallic reflection in which the interaction of light with a metal is expressed by scattering by the conduction electrons. Frenkel[8] treats the interaction of light with a metal as the probability of photons penetrating or being reflected by a surface potential barrier.

In two recent studies,[9,10] surface gas layers were used to explain the observed variations of vaporization rate and resistivity of tungsten. However, if such gas layers were present in this reflectivity study, they had no observable effect.

It seems possible that the electrostatic fields

TABLE I. Tests for a variation of reflectivity of tungsten filament with surface voltage gradient. Test No. 6. Measurements with special optical pyrometer; vacuum chamber irradiated with radium source; background lamp current constant at 3.8 amp. d.c.; high voltage voltmeter directly across test chamber terminals (360-megohm damping resistance).

Applied potential difference kilovolts	Gradient at filament 10^8 volts/cm	Lamp voltage for 6 pyrometer balances Max.	Min.	Av.	Average brightness of filament[a]	Average deviation of brightness measurement, percent	Range of measured brightness or reflectivity, percent
		Without Ra irradiation					
0	0	91.8	89.5	90.6	1.003	2.5	8.4
		With Ra irradiation					
0	0	91.8	89.5	90.5	1.000	2.4	8.4
3.96	1.07	92.5	90.0	91.2	1.026	2.7	9.0
7.91	2.15	92.0	89.8	91.0	1.018	2.5	8.1
11.87	3.22	91.8	89.5	90.8	1.011	2.5	8.3
15.82	4.28	92.2	89.8	90.9	1.015	2.7	9.0
19.78	5.36	92.0	89.5	90.7	1.008	2.9	9.1
23.90	6.48	91.0	90.5	90.8[b]	1.011	0.9	1.9
0	0	91.0	89.8	90.2	0.992	1.1	4.3
23.90	6.48	Test stopped due to filament vibration.					

Range of average brightness or relative reflectivity for entire test =3.4 percent.
[a] Arbitrary units—based on initial zero gradient value with Ra irradiation as unity. Reflectivity is proportional to the average brightness.
[b] Two balances instead of six.

TABLE II. Summary of results of reflectivity vs. surface voltage gradient tests on tungsten filament.

Test No.	Gradient at filament 10^8 volts/cm	Average brightness of filament[a]	Average deviation of brightness measurement, percent	Range of measured brightness or reflectivity, percent
		Ordinary pyrometer		
1	0	1.00	5.6	23
	4.28	0.98	9.4	23
	8.65	0.98	9.4	23
	9.78	1.08[b]	—	—
2	0	1.00	8.0	13
	2.15	0.98	5.5	13
	4.28	1.01	9.2	20
3	0	1.00	3.5	6.2
	2.15	1.00	3.5	6.2
	5.36	0.98	1.8	6.2
		Special pyrometer		
4	0	1.00	1.3	5.0
	3.22	1.00	3.5	12.
	5.36	1.00	4.4	12.
	6.00	0.98[c]	3.6	10.
5	0	1.00	1.3	5.9
	2.15	1.00	1.7	12.
	3.22	1.04	3.3	5.8
	4.28	1.03[c]	0.8	2.4
6	0	1.00	2.4	8.4
	2.15	1.02	2.5	8.1
	5.36	1.01	2.9	9.1
	6.48	1.01[d]	0.9	1.9

[a] Arbitrary units based on average value at zero gradient as unity. Reflectivity is proportional to the average brightness.
[b] One pyrometer balance instead of five.
[c] Four pyrometer balances instead of six.
[d] Two pyrometer balances instead of six.

[7] L. I. Schiff and L. H. Thomas, Phys. Rev. **47**, 860–869 (1935).

[8] J. Frenkel, *Wave Mechanics* (Oxford University Press, New York, 1932).

[9] P. L. Vissat, Ph.D. Thesis, University of Pittsburgh (1941).

[10] W. P. Reid, Ph.D. Thesis, University of Pittsburgh (1942); and Phys. Rev. **63**, 359–366 (1943).

used in the vaporization and reflectivity studies have not been able to modify with certainty the surface structure of the metal. The indications are that in extremely high vacuums certain changes in the vaporization rate and in the reflectivity of a metal should be produced by the application of sufficiently high electrostatic fields to the metal surface. In the case of reflectivity, in order to observe such effects, an improved form of apparatus would probably be required.

ACKNOWLEDGMENT

The author wishes to express his gratitude to Dr. Elmer Hutchisson, who suggested this problem and under whose guidance the research was started; to Dr. A. G. Worthing, who acted as advisor during the absence of Dr. Hutchisson in the present emergency, and made helpful suggestions in the preparation of the manuscript; and to Dr. A. J. Allen and other members of the Physics Department who offered suggestions.

PHYSICAL REVIEW VOLUME 65, NUMBERS 9 AND 10 MAY 1 AND 15, 1944

Letters to the Editor

PROMPT publication of brief reports of important discoveries in physics may be secured by addressing them to this department. The closing date for this department is the third of the month. Because of the late closing date for the section no proof can be shown to authors. The Board of Editors does not hold itself responsible for the opinions expressed by the correspondents. Communications should not in general exceed 600 words in length.

Note on Events Distributed According to Chance

ARTHUR E. RUARK
University of North Carolina, Chapel Hill, North Carolina
April 17, 1944

IN a recent paper[1] I have shown how to calculate the chance W_n that n events will occur in a domain of several dimensions described by variables x, y, etc. W_n can always be found if we are given the chance $f(x, y)dxdy$ that an event will occur in $dxdy$. In this note, I wish to record a development which arose in a problem dealing with surface flaws and volume flaws in glass and other brittle materials. It turns out that the method can easily be extended to give us the chance W_n that n flaws will be found in the volume V and on the surface S of a specimen. Let f be the volume density of interior flaws and f' the surface density of flaws on the boundary (which may be of the same kind, or of a different kind). Then, if f and f' are *constant*, we find, putting $fV+f'S=b$, that $W_n=b^n e^{-b}/n!$ This Poisson formula will be obvious to those who happen to be familiar with the result of superimposing random distributions, dependent on a single variable, but perhaps not so obvious to the majority of physicists interested in the faults of brittle materials. For more general cases, where f and f' are not constant, differential equations analogous to those in the above-mentioned paper have been set up. The methods of integrating them are in general the same as in the previous paper.

I take this opportunity to correct an error in the above-mentioned paper; a minus sign is needed in the second line below Eq. (10).

[1] A. E. Ruark, Phys. Rev. 65, 88 (1944).

The Decomposition of Water by the So-Called Permanent Magnet and the Measurement of the Intensity of the Magnetic Current

FELIX EHRENHAFT
New York, New York
April 28, 1944

THE magnetic current manifests itself in many phenomena. The polar movement[1] of bodies in an homogeneous magnetic field, reversing their direction of movement with the reversal of the field, showing that they bear an excess of north or south magnetic charge, constitutes a magnetic current. Thus the Peregrinus experiment becomes positive when performed with sensitive means. The well-known breaking experiment quoted by Maxwell[2] that a magnet when broken *ad infinitum* invariably gives always two separate magnets with equal poles cannot be found in the scientific literature, and it cannot be performed. This idealistic experiment does not prove that there is no true magnetism, north or south, because each breaking creates constriction, and from each constriction there is produced magnetism.

The decomposition of water into oxygen and hydrogen by the electromagnet[3] and the circulation of positively or negatively charged bodies and bubbles in the same plane, and at the same time, in directions opposite to one another, in the constant homogeneous vertical magnetic field, reversing their direction of circulation with the reversal of the field,[4] proves the existence of the magnetic current by the same criteria from which the existence of the electric current was deduced.

It has been observed that electrically evolved hydrogen bubbles in dilute acid, and iron hydroxide particles in a solution of iron chloride bearing a positive charge circulate counterclockwise, while electrically evolved oxygen bubbles in dilute acid, and copper particles in a solution of copper sulphate bearing a negative charge move clockwise when looking on the face of the south pole of the electromagnet. Of course there can be circulation of the liquid itself if it bears charges. This also proves the existence of the magnetic current.

Water can be decomposed also by the permanent magnet, and the fact that it loses a portion of its pole strength in the magnetolytic process gives us the possibility of measuring the intensity of the magnetic current. The magnet and cell used in these experiments are shown in Fig. 1. A semicircular Alnico Blue Streak magnet with outer radius of 5.1 cm, 1.75 cm thick, was used. Two pole pieces of soft Swedish iron are fitted to it, one electrically insulated from the magnet by a piece of paper. A metallic connection between the two poles is shown. The pole pieces are fitted into a glass cell through rubber gaskets. This cell is divided into two equal parts by a glass partition pierced with four holes plugged with asbestos, so that while there is a liquid contact between the two parts, the gases evolved could be collected separately from the two poles. In another arrangement two magnets were used. In this case the magnets are in a horizontal position, the two north poles against one pole block, and the two south poles against the other. These two arrangements, because of the fact that the poles were metallically connected, give in effect one piece of iron with the ends in the solution. A 4 percent solution of sulphuric acid by volume was used.

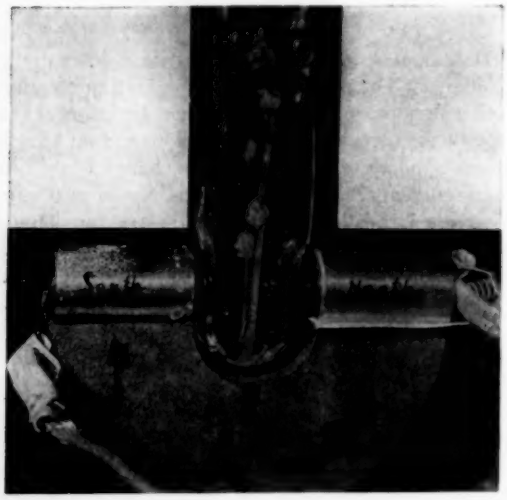

FIG. 1. Alnico blue steel magnet. Outer radius 51 mm, inner radius 15.8 mm, thickness 17.5 mm. Pole pieces are of soft Swedish iron having circular cylindrical extensions 10 mm in diameter, 12.5 mm long, and terminate in a truncated cone 6 mm in diameter. The circulation of gas bubbles is counterclockwise as one looks at the south pole.

Four points should be emphasized. First, the volume of gases evolved under identical conditions is greater when the magnetic field is applied than when the hydrogen is being formed by chemical action in its absence—in one case an 8.3 percent increase was noted. This increase in volume was also noted in experiments with the electromagnet. Second, when the magnetic field is applied, pure hydrogen is no longer evolved, but a mixture of oxygen and hydrogen comes from both poles, and in every case a greater percentage of oxygen comes from the north than from the south pole. In three cases it was 1.43 percent and 1.12 percent, 0.87 percent and 0.57 percent, and 0.25 percent and 0.16 percent, respectively. This is a proof that magnetism is polar. Since the field strength of the permanent magnet was less than one-tenth of that employed with the electromagnet, where two to twelve percent of oxygen in the mixture of gases was found, it appears from this and other observations that the percentage of oxygen evolved depends on the field strength and the acidity.[5]

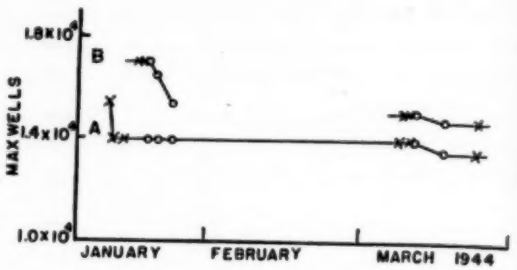

FIG. 2. Measurements of the strength of the Alnico magnet.

Third, the magnets *A* and *B* used in these experiments lost a considerable portion of their pole strength during the time of the magnetolytic processes. In Fig. 2 the pole strength is plotted against time. Before and after each magnetolytic process it was determined by search coil and ballistic galvanometer controlled by a simple method of the author that the flux value of the magnets was at a steady state.[6] The two magnets were used in separate tests in January. *A* lost about 1500 maxwells in 24 hours, and *B* lost 1600 in 108 hours. Two months later *A* and *B* were used in combination as described above, and the two together lost a total of 670 maxwells in 101 hours. From these figures one can readily calculate the loss in gauss per second, which gives at once the average intensity of the magnetic current flowing between the pole faces in absolute magnetostatic units. In the practical system, if one defines the unit as is done in electrical measurements, i.e., 3×10^{9} larger, the intensity of the magnetic currents, measured in practical units, will be as follows: In the first case 9.4×10^{-13}, in the second, 2.2×10^{-13}, and in the third 1.0×10^{-13}.

The fourth point is that while water was being decomposed as evidenced by the appearance of oxygen in the evolved gases and the permanent magnets lost a portion of their pole strength, further evidence of the expenditure of energy by the magnet is given by the observation of the circulation of gas bubbles around the axis of the horizontal magnetic field. These bubbles could be seen even

by the naked eye to be circulating in a counterclockwise direction, when looking upon the face of the south pole. This movement carried them downwards, even against the force of bouyancy.

Referring to the above-mentioned circulation of bubbles with the electromagnet, it is clear that the bubbles are charged electrically in this case also.

Until now it has been formulated that only a stream of electrostatically charged bodies or matter—the so-called convection current—moving at such great speed that it creates its own magnetic field can be influenced by an external magnetic field (Rowland-corpuscular rays). But now there is evidenced a force exerted by the magnetic field on electrostatically charged matter substantially at rest. The observation of the circulating bubbles is the inverse case of Oersted's experiment. He found that a magnetic needle was deflected by a wire connecting the poles of Volta's pile. This was interpreted by Ampere as the circulation of a single magnetic pole around the wire carrying an electric current. The phenomena herein described show that a single electric charge circulates around the magnetic current.

It is the belief today that there exist in nature only two general forces, the force of gravity and the magnetic action of electric currents (Oersted, Biot-Savart, Lorentz).[7] But we have here a third force, the electric action of magnetic currents. The intensity of the magnetic current has been measured magnetically. From this third force it becomes possible to define the intensity of the magnetic current electrically by the equation

$$\int_0 E ds = I_m.$$

Oersted found, to use his own words, a vortex around the wire connecting the two poles of Volta's pile. The phenomena here reported show that there is a vortex around the poles of an electro- or permanent magnet. In Oersted's experiment, the pile lost its pole strength. In the experiment with the permanent magnet, the magnet lost its pole strength. In Oersted's experiment, we have to deal with electrodynamic rotations. In the new case, we have to deal with magnetodynamic rotations. Both rotations are the result of the expenditure of energy, one from Volta's pile, the other from the magnet.

If the single magnetic pole is fixed and alone in action, the opposite pole being remote, as is done in Faraday's experiment, and the wire conducting the electric current is free to move, the wire will rotate around the single pole. This is the principle of the electric motor. Conversely, in accord with the principle of action and reaction, if the wire conducting the electric current is fixed, and the single magnetic pole is free to move, we also have an electric motor.

In the new case, in comparison with the last example, we have two fixed magnetic poles, with the electrically charged matter free to rotate around the magnetic current. This is, *in principio*, the magnetic motor. We are here using our third force. One cannot tell how a motor operated by this force can be utilized, but this is not our immediate concern. Of greater importance is the necessity to define more clearly the part that the inseparable twins, electricity and magnetism, play in their interaction, one on another, and to determine if, in the future, they can best be defined by one symbol only.

[1] F. Ehrenhaft, Comptes rendus **190**, 263 (1930); Physik. Zeits. **31**, 478 (1930); Phil. Mag. **11**, 140 (1931); Ann. de physique **13**, 151 (1940); J. Frank. Inst. **230**, 381 (1940); *ibid.* **233**, 235 (1942); Nature **147**, 25 (1941); Science **94**, 232 (1941); *ibid.* **96**, 228 (1942); E. Reeger, Zeits. f. Physik **71**, 646 (1931).

[2] J. C. Maxwell, *Treatise on Electricity and Magnetism* (Ed. Oxford, 1873), 377–379, etc. F. Ehrenhaft, J. Frank. Inst. **233**, 242–243 (1942).

[3] F. Ehrenhaft, Phys. Rev. **63**, 216, 461 (1943).

[4] F. Ehrenhaft, Phys. Rev. **63**, 461 (1943); **64**, 43 (1943); **65**, 62, 256 (1944).

[5] The chemical analyses were made by Foster D. Snell, Inc., Brooklyn, New York in the presence of the author and Richard Whitall. The determinations were made using alkaline pyrogallol in a Hempel pipet.

[6] Measurements by search coil and ballistic galvanometer (Rawson fluxmeter) were made by H. O. Nilsson of the Nilsson Electrical Laboratories, Inc., New York City, and also by the author and Richard Whitall.

[7] H. A. Lorentz, Encycl. d. Math. Wiss. **5**, 2, 156. A. Becker, *Theorie der Electricitat, Vol. II, Electronentheorie* (Neubearbeitete auflage von Max Abraham, 1933).

Note. The author wishes to thank Richard Whitall for his kind assistance in measuring by a potentiometer the potential differences between the pole pieces. These were found to occur in every experiment, usually of the order of 0.001 volt or less. In experiments where the poles were not metallically connected, analysis showed that oxygen was evolved.

On the Mixed Meson Theory of Nuclear Forces

J. M. JAUCH, *Princeton University, Princeton, New Jersey*
AND
NING HU, *Institute for Advanced Study, Princeton, New Jersey*

April 21, 1944

SCHWINGER'S[1] modification of the Møller-Rosenfeld[2] mixture of a pseudoscalar with a vector meson has been investigated quantitatively. In this theory the masses κ and μ of the pseudoscalar and vector mesons, respectively, are assumed to be different ($\kappa < \mu$), thus leaving open the possibility for an unstable vector meson with a lifetime of the order of 10^{-6} sec., the value required for the meson theory of the β-decay.[3] The observed lifetime of the cosmic-ray mesons of 2×10^{-6} sec. would then be almost exclusively due to the pseudoscalar mesons. With this theory inadmissible singularities in the tensor force are removed if the values of the coupling constants of the dimension of a length are assumed to be the same for the two kinds of mesons. Moreover, the tensor force has the correct sign so

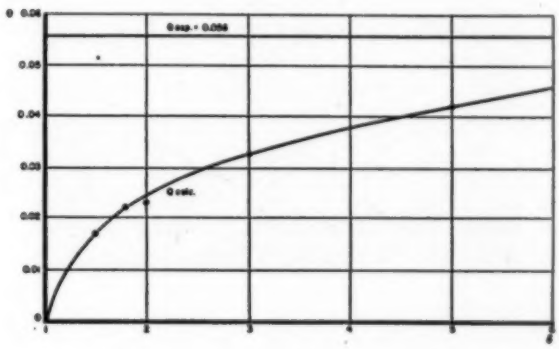

FIG. 1. The quadrupole moment Q for the deuteron in arbitrary units as a function of the mass ratio $\delta = \mu/\kappa$.

as to lead to a positive value of the electric quadrupole moment of the deuteron.

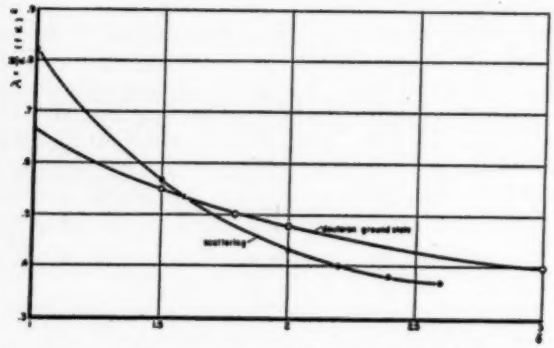

FIG. 2. The coupling constant as calculated from the binding energy of the deuteron and the scattering of slow neutrons on protons plotted as a function of the mass ratio $\delta=\mu/\kappa$.

For the static case (nucleons at rest) the force between two nucleons A and B is in this theory

$$V=\tfrac{1}{4}f^2(\tau_A\tau_B)\{J(r)(\sigma_A\sigma_B)+K(r)S_{AB}\}$$

with

$$J(r)=\kappa^3\frac{e^{-\kappa r}}{r}+2\mu^2\frac{e^{-\mu r}}{r},$$

$$K(r)=\frac{1}{r^3}(3+3\kappa r+\kappa^2r^2)e^{-\kappa r}-(3+3\mu r+\mu^2r^2)e^{-\mu r},$$

$$S_{AB}=\frac{3}{r^2}(\sigma_A\mathbf{r})(\sigma_B\mathbf{r})-(\sigma_A\sigma_B),$$

where σ and τ represent the operators of spin and isotopic spin of the nucleons.

There are essentially two constants at our disposal f and $\delta=\mu/\kappa$. The value of κ is taken from cosmic-ray measurements to be 177 m. The purpose of this calculation was to adjust the constants f and δ so as to fit the experimental values of (a) the binding energy of the deuteron in the ground ($3S$) state $E_0=2.17$ Mev; (b) the value[4] of the quadrupole moment of the deuteron $Q=2.73\times10^{-27}$ cm^2;[1] (c) the cross section $\sigma=14.8\times10^{-24}$ cm^2 for low energy $N-P$ scattering.[5] For the calculation of (a) and (b) the solution of the following coupled system of differential equations is required.[6]

$$u''+j(x)u+\sqrt{2}k(x)v=\epsilon u,$$

$$v''-(6v/x^2)+(j(x)-k(x))v+\sqrt{2}k(x)u=\epsilon v,$$

where

$$j(x)=f^2M\kappa(1/x)(e^{-x}+2\delta^2e^{-\delta x}),$$

$$k(x)=2f^2M\kappa(1/x^3)(x^2+3x+3)e^{-x}-(\delta^2x^2+3\delta x+3)e^{-\delta x},$$

$$\epsilon=ME_0/\kappa^2=0.25.$$

The numerical integration of this system is best carried out after the transformation to the new variable $\xi=1-e^{-x}(0<\xi<1)$. The boundary conditions for the bound state are then $u(0)=v(0)=u(1)=v(1)=0$.

Writing this system as a difference equation, we obtained an accuracy of ~2 percent for the coupling constant and quadrupole moment with five equidistant points in the variable ξ. The accuracy was estimated by taking ten and twenty equidistant points for ξ.

The coupling constant was first calculated for various values of δ ranging from 1 to 5. The magnitude of the quadrupole moment is then determined from the formula

$$Q=\frac{\sqrt{2}}{10}\int_0^\infty x^2\left(uv-\frac{1}{2\sqrt{2}}v^2\right)dx$$

for normalized functions:

$$\int_0^\infty(u^2+v^2)dx=1.$$

The result is plotted in Fig. 1. It is seen that the experimental value is considerably higher for reasonable mass ratio ($\delta<10$). The introduction of a coupling constant with longitudinal mesons does not improve the result. It was, however, recently pointed out by Hulthén[7] that the non-static forces give an appreciable contribution to the value of Q so that the disagreement of these calculations with the experiment is not sufficient evidence to disprove the theory.

It is, therefore, of some interest to fix the coupling constant and mass ratio from the conditions (a) and (c). The result is plotted in Fig. 2. The values $f\kappa=0.226$ and $\delta=1.6$ lead to the correct binding energy and scattering intensity. For these values of f and δ the static part of Q turns out to be $Q_{\text{stat}}=0.926\times10^{-24}$ cm^2. We are indebted to S. F. Singer for assistance in the numerical work.

[1] J. Schwinger, Phys. Rev. **61**, 387A (1942).
[2] C. Møller and L. Rosenfeld, Kgl. Danske Vid. Sels. Math.-Fys. Medd. **17**, 8 (1940); C. Møller, *ibid.* **18**, 6 (1941).
[3] L. Nordheim, Phys. Rev. **55**, 506 (1939).
[4] J. M. B. Kellogg, I. I. Rabi, N. F. Ramsey, and J. R. Zacharias, Phys. Rev. **57**, 677 (1940); A. Nordsieck, Phys. Rev. **58**, 310 (1940).
[5] L. Simons, Phys. Rev. **55**, 792 (1939).
[6] W. Pauli and S. Kusaka, Phys. Rev. **63**, 412 (1943), Eq. (114).
[7] Hulthén, Arkiv f. Mat. Astronom. Fys. **29A** (1943).